FEBS Letters

FEBS PRESS science publishing by scientists

REVIEW

Photosynthesis under far-red light—evolutionary adaptations and bioengineering of light-harvesting complexes

Antonello Amelii[1], Edoardo Andrea Cutolo[1], Daniele Montepietra[1], Claudia Battarra[1], Roberto Caferri[1], Stefano Capaldi[1], Zeno Guardini[1], Luca Dall'Osto[1] and Roberto Bassi[1,2]

1 Laboratory of Photosynthesis and Bioenergy, Department of Biotechnology, University of Verona, Italy
2 Stazione Zoologica Anton Dohrn Napoli, Naples, Italy

Correspondence
R. Bassi, Laboratory of Photosynthesis and Bioenergy, Department of Biotechnology, University of Verona, Strada Le Grazie 15, 37134, Verona, Italy
Tel: +39 0458027916
E-mail: roberto.bassi@univr.it

(Received 15 May 2025, revised 12 September 2025, accepted 22 September 2025, available online 28 October 2025)

doi:10.1002/1873-3468.70191

Edited by Peter Brzezinski

In plants and algae, photosynthesis is driven by the absorption of sunlight energy by networks of pigments housed within light-harvesting proteins. Special photosynthetic complexes can intercept the low-energy photons corresponding to the far-red spectrum of the photosynthetically active radiation. These so-called red chlorophyll forms are found in multiple lineages of the Viridiplantae clade, are formed upon a change in spatial organization of chromophores within specific subunits of the photosystem I supercomplex, and can be detected by their unique red-shifted fluorescence emission signatures. Red forms enabled phototrophs to colonize light-limited ecological niches, especially where far-red radiation is enriched by leaf shading. The protein environment plays a key role in determining the occurrence of red forms, promoting strong excitonic interactions among chlorophyll *a* molecules and facilitating their excitation by low-energy photons. In this review, we present a comprehensive account of the evolutionary diversity of long-wavelength-driven photosynthesis in eukaryotes, and detail the biophysical and structural determinants of this phenomenon. Finally, we discuss how this knowledge can be applied in biotechnology to engineer crop canopies with broadened light absorption and higher yield potential.

Keywords: chlorophyll; excitation energy transfer; far-red light; light-harvesting; photosynthesis; protein engineering; structural biology

Introduction

Solar radiation drives the photosynthetic reactions that convert light into chemical energy, thereby supporting life on Earth. Evolution optimized the light-harvesting apparatus of phototrophs to function according to the spectral conditions found on land and in aquatic habitats [1–4]. In land communities, shading between neighboring plants strongly influences light availability. The upper canopies sequester the red and blue photons and only transmit 1–2% of the incident photosynthetically active radiation (PAR; 400–750 nm) to the forest floor, mainly consisting of the poorly absorbed green and far-red (FR) wavelengths (Fig. 1A) [5]. Similar steep light gradients are also found within high-density crop monocultures: following closure, the top canopy is exposed to full irradiance, while the lower foliage experiences constant light limitation. This is also

Abbreviations
Car, carotenoid; CC, core complex; Chl, chlorophyll; Ct, charge transfer; EC, excitonic coupling; EET, excitation energy transfer; FR, far-red light; HOMO, highest occupied molecular orbital; LHCI/II, light-harvesting complex I/II; LUMO, lowest unoccupied molecular orbital; PAR, photosynthetically active radiation; PSI/II, photosystem I/II; R:FR, red to far-red ratio; RC, reaction center; RF, red form; SC, supercomplex.

FEBS Letters **600** (2026) 164–187 © 2025 The Author(s). *FEBS Letters* published by John Wiley & Sons Ltd on behalf of Federation of European Biochemical Societies.

accompanied by a downward decrease of the red-to-FR ratio (from 1.2 at the top down to 0.1 at soil level), which limits productivity [6–10].

In eukaryotic phototrophs, two photosystems [photosystem I (PSI) and PSII] harvest photons through an antenna system consisting of light-harvesting complex (LHC) proteins that bind chlorophyll (Chl) *a*, Chl *b*, and xanthophylls (Xan). Whereas Chl *a* is present both in the core complexes (CCs) and the peripheral antenna, Chl *b* is only found in the antenna systems [17]. The absorbed energy is funneled to the reaction centers (RCs) of PSI and PSII, where it activates photochemical reactions, initiating a linear flow of electrons along the thylakoid membranes [1]. Electron transport is driven by PSI and PSII, which operate in series, ultimately reducing $NADP^+$ to NADPH (Fig. 1C) and sustaining ATP through the building of a trans-thylakoid proton gradient [18]. PSI and PSII have distinct spectral properties (Fig. 1E): whereas PSII predominantly intercepts blue and red photons, PSI possesses red chl forms or red forms (RFs), which extend its light-harvesting capacity to cover the longest PAR wavelengths ($\lambda \geq 700$ nm) [19]. Both the PSI core and in its antenna system exhibit a distinct red-shifted absorption compared to PSII, a property inherited from the cyanobacterial ancestors [20]. The PSI antenna system (LHCI belt) of higher plants consists of two Lhca heterodimers and binds $\sim$60 Chl molecules (Fig. 1F). These include the RFs, strongly interacting low-energy Chl pairs absorbing beyond the P700 PSI RC [21–24]. Although RFs account for a small fraction (4–5%) of photon interception under full sunlight, they contribute up to 40% to photon absorption in shade [25–27]. Therefore, understanding the structural and biophysical determinants of RFs may provide a blueprint for designing light-harvesting systems tuned for optimal use of FR light and enhanced photosynthesis in high-density crop monocultures.

Far-red light in plant physiology

The Viridiplantae clade—or green lineage—emerged 1 billion years (Ga) ago. It then witnessed the transition of multicellular phototrophic eukaryotes from marine to land habitats around 500 million years (Ma) ago, and the explosion of angiosperm biodiversity around 110 Ma [28–37]. Land colonization prompted organisms to adapt to greater environmental variability and a broader light spectrum, leading to competition for photon intercepting. In plants, this was achieved by developing complex canopy architectures and through the expansion of the LHC repertoire to include isoforms optimized for FR light absorption [38–48]. FR light regulates multiple processes in plant physiology [49,50]. In the short term, FR light adds to red and blue light in synergistically driving photosynthesis (Emerson enhancement effect) [51–57] and controls the balancing of PSI *vs.* PSII excitation via reversible post-translational modifications of LHCs [58]. In the long term, acclimation to FR light causes the reprogramming of pigment metabolism and the adjustment of the chloroplast architecture and of the light-harvesting apparatus. This includes changes in the PSI/PSII stoichiometry and in the expression of

Fig. 1. Light spectrum in terrestrial and aquatic habitats, overview of the light reaction of photosynthesis and structure of PSI and PSII supercomplexes. (A) Solar irradiance spectrum at midday recorded at the canopy top (orange) and in the understory (red) (own data). (B) Attenuation of solar irradiance in the water column with depth. This figure was created using data reported in 11. The black (A) and red (B) traces show the absorption spectrum of an *Arabidopsis thaliana* leaf. (C) Schematic overview of the photosynthetic complexes in the thylakoid membrane. Photosystem II (PSII; PDB: 5XNM [11]) captures light energy and catalyzes the oxidation of water, releasing oxygen and transferring electrons to the plastoquinone (PQ) pool. Electrons are transferred to the cytochrome b_6f complex (Cyt b_6f; PDB: 6RQF [12]), plastocyanin (PC; PDB: 1PNC [13]), and finally to photosystem I (PSI; PDB: 9GBI), which uses additional photon energy to reduce ferredoxin (Fd; PDB: 1A70 [14]). Ferredoxin–$NADP^+$ reductase (FNR; PDB: 1FNC [15]) catalyzes the final step in NADPH formation. Electron transfer is coupled to proton translocation across the membrane, generating a proton gradient that powers ATP synthesis via the ATP synthase complex (PDB: 6FKF [16]). The core complexes of PSI and PSII, where charge separation occurs, are associated with peripheral light-harvesting antennae that enhance photon capture. Whereas the core complexes are highly conserved, the antenna composition varies across photosynthetic lineages. This figure was created with BioRender.com. (D) Structural model of the plant PSII–LHCII supercomplex (PDB: 5XNM), top view. The PSII core complex (Core; gray) is surrounded by peripheral light-harvesting complexes, including the LHCII trimers and the minor antenna proteins (Lhcb4–6). (E) Absorption spectra of isolated PSII–LHCII ($C_2S_2M_2$; blue) and PSI–LHCI (red) supercomplexes from *A. thaliana*. PSI–LHCI displays enhanced long-wavelength absorption compared to the PSII–LHCII (own data, $n = 3$). (F) Structural model of the plant PSI–LHCI supercomplex (PDB: 4XK8), top view. The PSI core complex (Core; gray) is surrounded by the LHCI antenna belt, composed of Lhca1–4 heterodimers (Lhca1 and 4: blue, red; Lhca2 and 3: magenta, orange). Bound chlorophylls and carotenoids are shown in green in panels (D) and (F). The structural models were created using the PyMOL Molecular Graphics System, Version 3.0 Schrödinger, LLC.

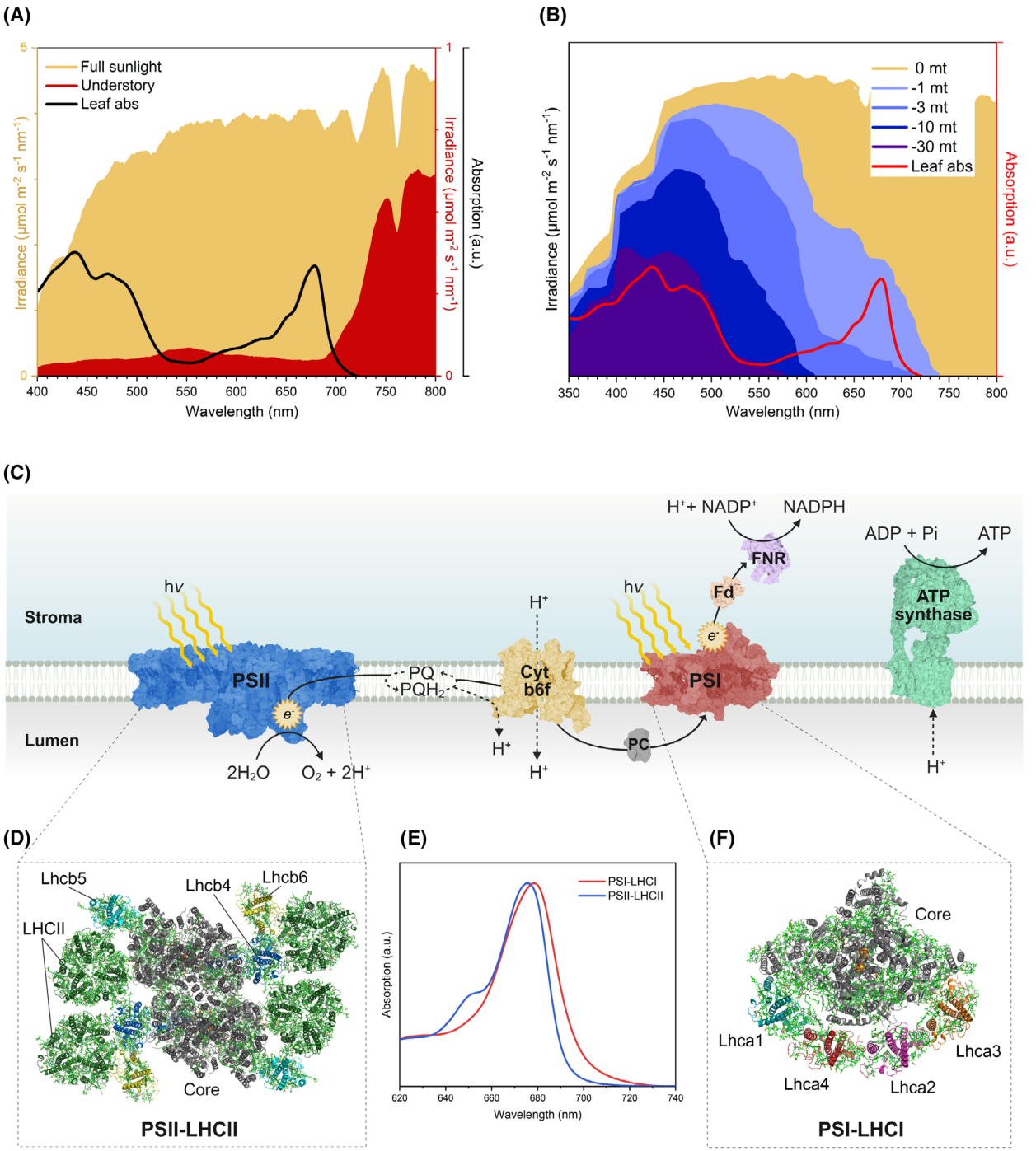

specific LHC isoforms [45,59–64]. Over an even longer time frame, FR light acts as a photomorphogenic signal that activates shade-avoidance growth responses [65–68]. Therefore, the pleiotropic effects of FR light need to be carefully considered when testing the effect of different light regimes on plant growth responses [69–71].

Occurrence of red forms in eukaryotic phototrophs

RFs have been identified within the PSI supercomplex (SC) of most lineages of eukaryotic phototrophs. In contrast, in prokaryotes, RFs primarily result from specific red-shifted Chl types synthesized during

acclimation to FR light, which are incorporated into the CC of both photosystems (for a comprehensive review, see [72]). The evolution of eukaryotic RFs can be traced back to the Ordovician–Silurian period (approx. 489–403 Ma), corresponding to the diversification of vascular plants and the appearance of forest canopies [73–79]. Eukaryotic RFs arise from pigment-pigment and pigment–protein interactions within the LHCI belt [80–82], which, in virtually all higher plants, consists of the protein heterodimers Lhca1–Lhca4 and Lhca2–Lhca3 (Fig. 1F), and displays a characteristic fluorescence emission signature at ~730 nm at cryogenic temperature (77 K). [22,83–85]. Specifically, the *A. thaliana* Lhca1–Lhca4 dimer displays fluorescence emission at 731.5 nm, whereas Lhca2–Lhca3 emits at 728.5 nm [43,86,87]. The *in vitro* analysis of recombinant (r)Lhca complexes pinpointed the origin of the red-shifted fluorescence emission peak to the Lhca3 (725 nm) and Lhca4 (733 nm) subunits, whereas rLhca1 and rLhca2 both emit at 702 nm [88–93]. Furthermore, the mutational analysis of rLhca subunits revealed that the absorption tail causing the red-shifted fluorescence emission in Lhca3 and Lhca4 originates from strong excitonic interaction of the Chl pair *a*603–*a*609, where the asparagine (Asn) residue coordinating Chl *a*603 emerged as the key structural determinant (described in more detail in Section 'The protein ligand') [43,94–95]. Both emission and absorption of LHCI subunits display a more pronounced red-shift when they are assembled in dimeric structures and when they are associated with the PSI CC [96]: the fluorescence emission λ_{max} of Lhca3 shifts from 725 nm to 728.5 nm when part of the Lhca2–Lhca3 dimer and to 735 nm in the fully assembled PSI–LHCI complex [86,87,97–100]. These effects derive from the combination of multiple factors, including pigment–pigment and pigment–protein interactions, which stabilize these low-lying energy states (discussed in Section 'Biophysical determinants') [101].

Plant evolution was accompanied by the constant expansion of PSI absorption toward longer wavelengths, and the progressive relocation of RFs from the CC to peripheral LHCI sites [25,26,37,84,98,102–105] (Fig. 2). Red-shifted emission spectra between 730 and 740 nm were recorded in land plants such as *Nicotiana tabacum* (Solanaceae), *Zea mays* (Poaceae), *Pisum sativum* (Fabaceae), *Spinacia oleracea* (Amaranthaceae), *Spathiphyllum wallisii* (Araceae), *Calathea roseopicta* (Marantaceae), and *Hordeum vulgare* (Poaceae) [98,99]. Greater shifts were observed in *Oryza sativa* (743 nm; Poaceae) and *Panax notoginseng* (747 nm; Araliaceae), and even more in the shade-tolerant species *Fittonia albivenis* (Acanthaceae), with λ_{max} values beyond 748 nm [100]. Intriguingly, the seagrasses *Posidonia oceanica* (Posidoniaceae) and *Cymodocea nodosa* (Cymodoceaceae) exhibit blue-shifted emission peaks at around 720 nm and 723 nm, respectively [106]. The loss of RFs in these species probably occurred because of the relaxed selective pressure following their return to the FR-deprived marine environment approx. 60 Ma (Fig. 1B) [107–110]. Furthermore, the PSI–LHCI emission λ_{max} values of most extant mosses (bryophytes) range between 717 and 735 nm [37,82,111]. Mosses are evolutionary intermediates between green algae and land plants and display early adaptations to land shade environments, including unique PSI features [29]. For instance, in *Physcomitrium patens*, the Lhca4 subunit is replaced by the paralog isoform Lhca2b. In Lhca2b, Chl *a*603 is coordinated by a histidine (His) residue, a modification that likely accounts for a ~10 nm shorter emission wavelength compared to the PSI–LHCI complexes of higher plants [37]. Instead, in the Lhca3 subunit, Chl *a*603 is coordinated by Asn like in angiosperms, suggesting that this feature was established during the adaptation to FR-light-enriched environments [82]. Another specific feature of *P. patens* is the Lhcb9 subunit found in the PSI–LHCI–LHCII megacomplexes, in which both Chls *a*603 and *a*612 are coordinated by Asn residues and display an emission peaking between 683 and 687 nm [112–116].

Blue-shifted PSI–LHCI fluorescence emission peaks are observed further up in the phylogenetic tree of phototrophic eukaryotes. For instance, the freshwater unicellular chlorophyte *Chlamydomonas reinhardtii* displays emission λ_{max} around 720 nm [104,117]. In this species, RFs are found in the outer LHCI belt, where the Lhca2, Lhca4, and Lhca9 subunits occupy a more distal position from the CC compared to the Lhca3 and Lhca4 plant isoforms. In these subunits, Chl *a*603 is coordinated via conserved Asn residues [81,104]; however, they display a blue-shifted emission peaking between 690 and 717 nm, respectively [117]. Similarly, in the marine chlorophyte *Ostreococcus tauri*, Asn residues coordinate Chl *a*603 in Lhca5 and Lhca6, but their emission λ_{max} peaks at ~700 nm [118], suggesting that other protein features influence their spectral responses [41,119].

Recently, additional types of RFs have been described in the eustigmatophyte *Trachydiscus minutus* [120]. In this species, a cluster comprising Chl *a* and two Xan molecules and exhibiting strong excitonic interaction is found in a specific class of LHCs known as violaxanthin–Chl *a* proteins [121,122]. Furthermore,

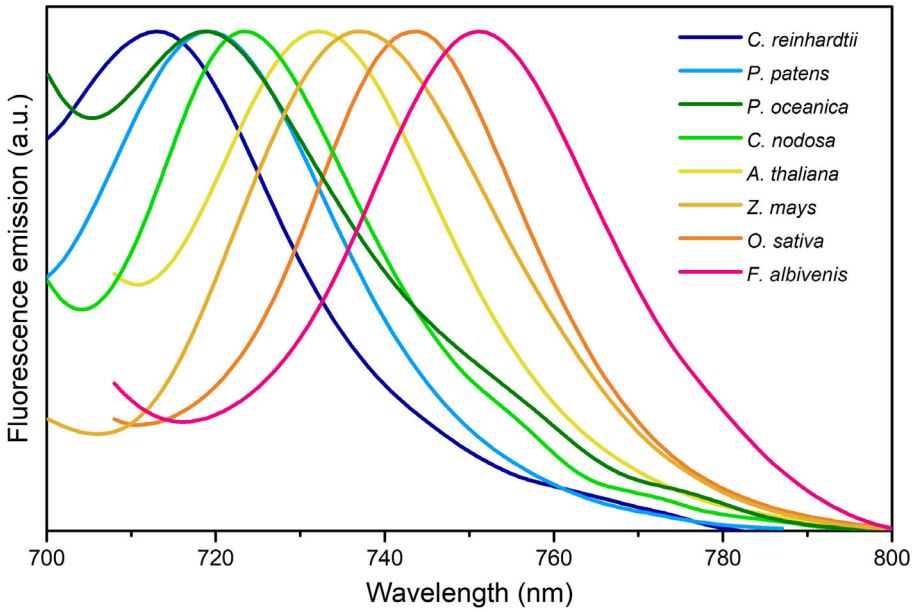

Fig. 2. Progressive extension towards the red spectrum of light-harvesting systems in the evolution of eukaryotic phototrophs. Fluorescence emission spectra were recorded at cryogenic temperature on leaf extracts and cell suspensions of representative species from phylogenetic groups. This figure was created using data from [106].

in the trebouxiophyte *Prasiola crispa*, a long-wavelength Chl *a* accumulates in its PSII–LHCII [123]. These features require the FR-light-induced expression of the *Pc-frLHC* gene, a divergent LHC isoform [124]. This type of acclimation response is observed in other phytoplankton taxa, as recently reported for the flagellate *Euglena gracilis*. In this case, pentameric complexes consisting of the taxon-specific FR-absorbing Lhce isoform associate with both PSI and PSII under low light following FR light acclimation [125–127]. Finally, in some diatoms and other eustigmatophytes, the occurrence of RFs appears to depend on additional factors other than pigment geometries, such as the Chl:carotenoid ratio of LHCs, highlighting the complex basis of low-energy photon absorption in photosynthesis [120,128–129].

Principles of low-energy absorption

Biophysical determinants

Chls are tetrapyrrole macrocycles that incorporate an Mg^{2+} ion, a phytol chain, and a characteristic fifth ring, together featuring an extended system of conjugated bonds that is responsible for two main absorption bands in the blue (Soret band) and red (Q band) regions of the visible spectrum. These bands comprise independent electronic transitions named Q_y (or S_1), Q_x (or S_2), and the Soret band (S_3), which is a superposition of the B_x and B_y bands, with the x and y annotations indicating the polarization directions within the macrocycle plane (Fig. 3A) [130]. In Chl *a*, the lowest (Q_y) and the second lowest energy (Q_x) absorption bands possess orthogonal transition dipole moments. These transitions are qualitatively described by the four-orbital model, which involves the two highest occupied molecular orbitals (HOMOs) and the two lowest unoccupied molecular orbitals (LUMOs) [131–133]. The Q_y transition can be expressed as a linear combination of the transition from HOMO to LUMO and from HOMO−1 to LUMO+1. In contrast, the Q_x transition is expressed as a linear combination of transitions from HOMO−1 to LUMO and from HOMO to LUMO+1 (Fig. 3C). The B_x and B_y transitions can also be expressed by linear combinations of the two transition dipole moments along the *x*- and *y*-axes, respectively (Fig. 3B) [134].

The absorption spectra of Chl-binding proteins exhibit significant heterogeneous broadening in the Q_y region (630–685 nm range) due to the presence of distinct spectral forms [136], which are attributed to the localization of Chls in different protein sites. The interactions between Chls *a* and their protein environment modulate the pigment absorption properties compared to organic solutions. These interactions cause spectral broadening and a shift of their absorption toward

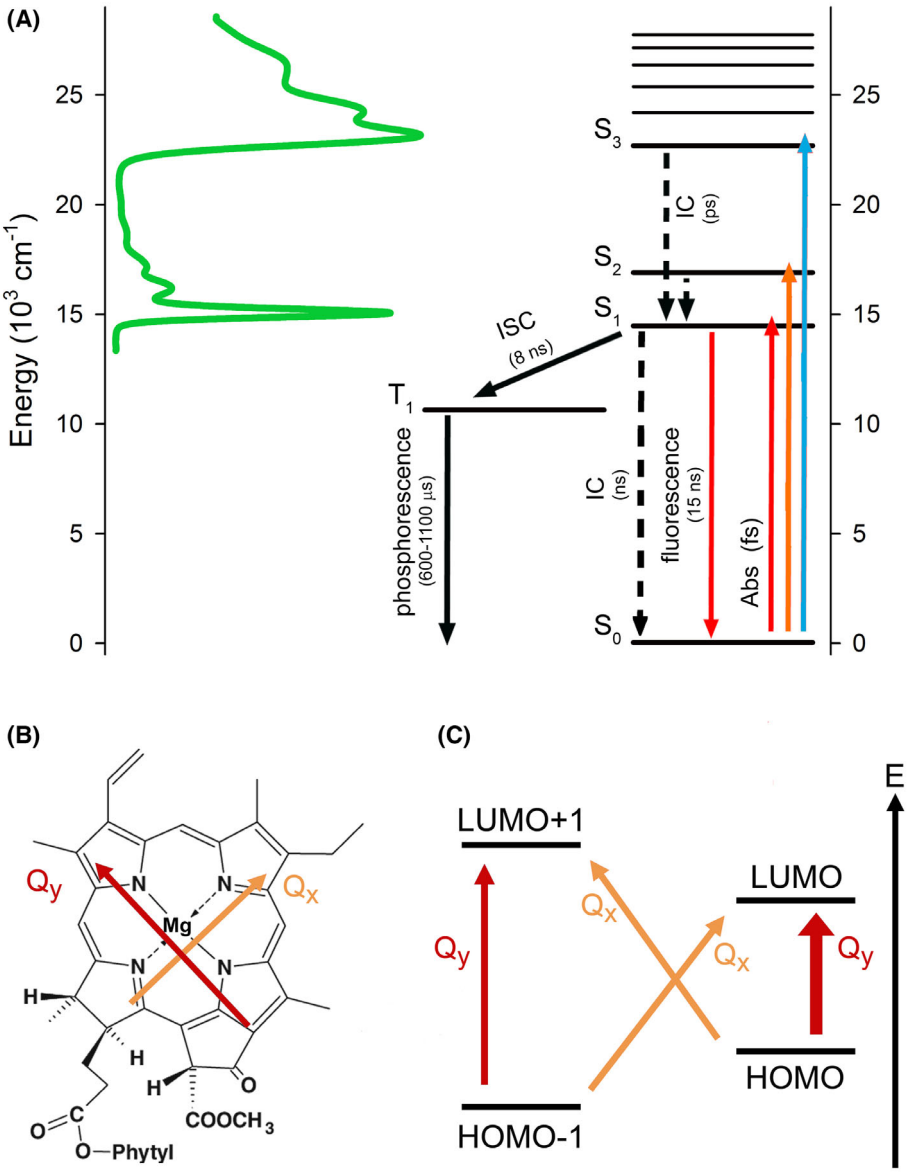

Fig. 3. Transition energy diagram of chlorophylls. (A) Chl *a* transition energy diagram. Excitation and relaxation processes are indicated by arrows and their corresponding time constants. The range of energies for pigment transitions is related to the visible absorption spectrum of the pigment. Abs, absorption; IC, internal conversion; ISC, intersystem crossing. (B) Chemical structure of Chl *a*. The red and orange arrows indicate the orientations of the Q_x and Q_y transition dipole moments, respectively. (C) Contributions of the Highest Occupied Molecular Orbital (HOMO), the second HOMO (HOMO–1), Lowest Unoccupied Molecular Orbital (LUMO) and the second LUMO (LOMO+1) to the Q_y and Q_x absorption bands. The Q_y transition is represented as a linear combination of transitions from HOMO to LUMO and from HOMO–1 to LUMO+1, whereas the Q_x transition is expressed as a linear combination of transitions from HOMO–1 to LUMO and from HOMO to LUMO+1. The thick red arrow indicates the main Q_y transition. This figure has been adapted from [134,135].

longer wavelengths (bathochromic shift) due to changes in electronic energy levels. Specifically, the Q_y band shifts from 664 nm in organic solvents to the 665–685 nm range observed in most Chl *a* molecules when bound to photosystems [137]. The arrangement of neighboring pigments can further shift Chl absorption into the red spectrum. For instance, some molecular interactions that produce RFs result in energy states lower than the primary photochemical trap of the PSI RC. This spectral red-shift arises from excitonic coupling, in which the excited states are delocalized over two or more pigments [92,138]. This coupling is highly sensitive to the environment, so slight structural differences in the host protein can alter the

geometry of pigment organization, bringing the Chls closer together. This enhances the probability of inter-pigment electron transfer processes, making charge transfer (CT) states more significant. Since the CT states are generally close in energy to the singlet-excited states of a Chl pair, they will tend to mix into the excited state. These events can significantly change the spectroscopic properties of pigment–protein complexes, leading to large homogeneous broadening, Stokes shifts, and strong electron–phonon coupling [92,139–140].

Excitonic coupling

Chls spaced closely together can form molecular excitons, which are excited electronic states involving more than one pigment molecule. Exciton energies result from the coupling between the excited states of individual pigments and are affected by their local environment—including nearby residues, protein electrostatics, and the medium. Although excitons are delocalized states, their properties depend on the energies of localized excitations and the interactions between them [141].

The electronic properties of pigment aggregates are commonly described by the Frenkel exciton model, in which the excitonic coupling (EC) can be decomposed into a long-range Coulomb contribution and a short-range term related to the orbital overlap between interacting chromophores (CT contributions) [142–144]. The exciton model typically neglects all CT contributions to the aggregate excited states. This simplification is justified by the fact that most interpigment distances are sufficiently small to enable significant EC, yet sufficiently large to prevent CT effects. By omitting CT contributions, a classical interpretation of the system can be provided, as the electrostatic interaction between two charge densities represents the excitations of the coupled chromophores [145].

EC becomes relevant when the interaction energy E_{ab} is proportional to or exceeds the energy difference between the individual pigments (*i.e.*, $E_{ab} > |E_a - E_b|$). Conversely, when excitonic mixing is moderate or minimal (i.e., $E_{ab} < |E_a - E_b|$), excitations are largely localized over one or more Chls that make up the aggregate, allowing the Förster equation to remain applicable. This is evident from the observation that the strongest EC between two Chls is $\sim 120\ cm^{-1}$, thus significantly smaller than the energy separation between the Q_y levels of these molecules ($\sim 450\ cm^{-1}$). ECs are quite stable and, therefore, less sensitive to changes of the internal geometry and orbital overlap of pigments. ECs are more strongly influenced by the relative position and orientation of pigments, since they are determined by the Coulomb coupling between transition dipole moments. By contrast, site energies can vary significantly with minor changes in molecular geometry [140].

Charge transfer

When pigments lie in proximity, the likelihood of electron transfer between them increases, making CT states significant. These CT states are polar in nature, exhibiting an excited-state dipole moment between the ground and excited states [92,146]. The dipole moment associated with CT states facilitates coupling between the optical transition and the (polar) phonon (i.e., quantum of vibrational mechanical energy) of the environment, thereby enhancing exciton–phonon coupling. Stark spectroscopy experiments revealed that the excitonic states of Chl *a* in LHCII probably behave in a similar way to those of unbound monomeric Chl *a* [147]. This indicates that there is little or no delocalization of the excitation, which would be expected in the case of strong EC [147].

The absorption spectrum of a pigment within a protein coordination site typically displays a narrow zero-phonon line, representing the pure electronic transition, along with a broad, blue-shifted phonon band associated with low-frequency vibrations of the protein matrix, coupled to the electronic transition [148]. Several factors influence the width of these absorption bands. For instance, the coupling of electronic transitions to vibrations of the pigments and the protein environment (phonons) leads to homogeneous broadening, which is temperature-dependent [149].

By contrast, inhomogeneous broadening arises from structural fluctuations within the protein matrix, leading to a Gaussian distribution of optical transition frequencies. This statistical distribution remains unaffected by temperature but is influenced by slow fluctuations that alter the pigment-binding sites [92,150]. The magnitude of CT couplings, which is directly related to the degree of molecular orbital overlap [140], is crucial for the occurrence of low-energy absorption and fluorescence emission signatures. By contrast, the energies of CT states, which are significantly higher than the exciton energies, primarily influence the precise positions of the red-shifted bands [140].

EC alone, however, does not fully account for the spectra of red-most LHC proteins, such as Lhca4, or for the broad bandwidth associated with RFs. For instance, the red-most transition of LHCII, which has a similar pigment organization but an interaction energy that is half that of Lhca4 ($120\ cm^{-1}$ *vs.*

260 cm^{-1}) is centered around 681 nm [92,149,151]. In Lhca4, both Chl *a*610–*a*611–*a*612 and *a*603–*a*609 pigment clusters are red-shifted. However, the lowest exciton level of the *a*603–*a*609 cluster lies further in the red spectrum due to mixing with the charge transfer state [95,138,140,152–155]. As suggested by recent quantum mechanics/molecular mechanic models focusing on the Lhca4 monomer, a larger component of CT displays *a*603 ➔ *a*609 directionality [106].

Excitation energy transfer

Within the LHC protein matrix, pigments create local funnels that convey the absorbed energy to the RCs through preferential routes [1,42,156]. Pigments exhibit different site energies, which are tuned by the interactions with neighboring chromophores and, in turn, govern the excitation energy transfer (EET) dynamics. RFs constitute energy valleys lying deeper than RCs that influence EET in PSI–LHCI, decreasing the overall trapping rate [157,158]. Significantly, the slow energetically uphill EET pathway from RFs in LHCI increases the trapping time by a factor of three: from ~22 ps to ~65 ps [86,87,159–160].

An important distinction exists between PSI antenna subunits with few but highly intense red clusters (Lhca3 and Lhca4) and those featuring multiple red clusters with higher energy levels (Lhca1 and Lhca2), in terms of EET and trapping times [158,161–162]. For instance, the red Lhca3 and Lhca4 isoforms are less efficient in transferring energy to the RC compared with the blue isoforms Lhca1 and Lhca2 (40 *vs.* 10 ps), with Lhca3 contributing approximately 40% to the increased trapping time in PSI–LHCI, whereas Lhca4 accounts for 60% [87].

In the antenna subunits that contain more isoenergetic Chl clusters (Lhca1 and Lhca2), excitons can populate several of the lowest energy sites after equilibration. For instance, the lowest exciton level of the Chl *a*602–*a*603–*a*609 cluster of Lhca1 is also red-shifted, albeit to a lesser extent than the same cluster of Lhca4. Furthermore, Lhca1 contains additional RFs as part of the Chl *a*610–*a*611–*a*612 cluster, as well as on its CC-exposed side, consisting of Chl *a*606 and the *a*613–*a*616 pair. Their coupling has been suggested to facilitate the depopulation of Lhca4, providing an alternative EET route to the CC [89,163].

It has also been proposed that low-energy clusters may exist within the PSII antenna system (Lhcb). For instance, within trimeric LHCII complexes, an efficient EET is facilitated by the presence of the red Chl cluster *a*610–*a*611–*a*612. Notably, Chl *a*610 has been identified as the red-most site, where energy is predominantly populated, thereby promoting a functional EET route towards other PSII subunits and the CC [42,164–168]. Another preferential EET route to the PSII RC involves two low-energy sites (*a*610–*a*611–*a*612/*a*602–*a*603–*a*609) located in the monomeric antenna Lhcb4, which create a structural and energetic bridge at the interface between the outer LHCII system and the CC (Figs 1D, 4) [169]. Instead, two Chl pools with energy levels lower than PSII RC (P680) are housed in the inner antenna subunits CP43 and CP47 of the PSII CC, which are characterized by fluorescence emission at 685 nm and 695 nm, respectively [170,171].

Structural determinants

The protein ligand

The identity of the amino acids that coordinate Chl *a*603 and *a*612 is a key factor in determining the occurrence of RFs in the Lhca subunits of *A. thaliana* (Fig. 5A) [43,95,140,172]. In the monomeric PSII antenna Lhcb4, two His residues are responsible for this coordination, and the absorption λ_{max} is 680 nm [169,173–174]. Conversely, in Lhca1 and Lhca2, where Asn residues coordinate Chl *a*612 and His residues coordinate Chl *a*603, λ_{max} is shifted to 702 nm. Lhca3 and Lhca4, however, feature two Asn residues coordinating Chl *a*603 and *a*612, resulting in a λ_{max} greater than 720 nm [95]. In *P. patens*, which has an Asn residue in Lhca3 and a His residue in Lhca4 as Chl *a*603-binding residues, a less red-shifted emission is observed compared to higher plants [43]. As previously mentioned, some angiosperms display different λ_{max} despite sharing the same ligands of the Chl pairs [98], probably as a consequence of the different orientations of the transmembrane helices and local protein environments, which affect the interactions between the bound pigments. Therefore, these interactions potentially make a more significant contribution to RF occurrence than the identity of the coordinating ligand [43]. Although the coordination of Chl *a*603 by Asn is not sufficient to confer significant FR absorption, it plays a critical role in maintaining the correct geometry between Chl *a*603 and *a*609, which is essential for the strong interaction in this cluster [43,84,140]. Indeed, when Asn is replaced by His or Gln, the corresponding RF is lost [43,95].

The protein environment

The protein scaffold that houses Chls influences directly and indirectly the width of the absorption bands of pigments. For instance, the environment may

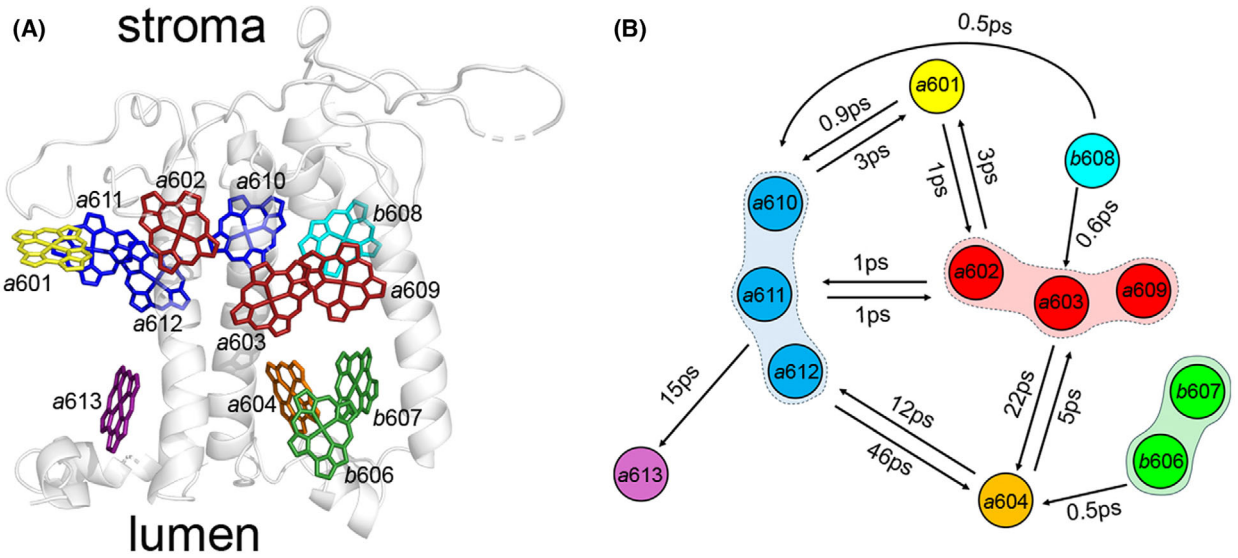

Fig. 4. Pigment topology and energy transfer pathways in the Lhcb4 subunit of photosystem II. (A) Illustration of the Chls embedded within the protein scaffold of the PSII monomeric antenna complex Lhcb4 (CP29). The structure is based on [169] and shows the nomenclature of Chls housed inside Lhcb4 and the complex orientation with respect to the thylakoid membrane. (B) Excitation energy transfer between the pigment domains of Lhcb4 based on [169].

include charged residues that promote hydrogen (H)-bonds between the amino acid side chains and pigment functional groups [43,176–177]. Moreover, the protein backbone stabilizes pigments, modulates their interactions, and provides vibrations at appropriate frequencies, bridging energy gaps between excitonic states that facilitate EET [1,84,150,178]. Notably, the protein environment of the red-shifted Chl cluster *a*603–*a*609 is different. Whereas Chl *a*609 is immersed in a charged environment via the coordination by glutamate (Glu) and an adjacent arginine (Arg), Chl *a*603 is mainly surrounded by apolar residues. It was suggested that the presence of bulky hydrophobic amino acids close to the Chl *a*603–*a*609 cluster of Lhca3 (phenylalanine–tryptophan–phenylalanine in place of glycine–phenylalanine–isoleucine) may contribute to the large red-shift in *F. albivenis* and other Acanthaceae (*e.g.*, *Strobilanthes cusia* and *Andrographis paniculata*) (Fig. 5B) [100]. The steric hindrance caused by the side chains of these hydrophobic residues appears to reduce the distance between the chlorine rings of Chls *a*603 and *a*609, promoting their stronger interaction [100]. In addition, the relative orientation between Chl *a*603–*a*609, combined with changes in the chemical and physical properties of the environment, might further reinforce the red-shifted fluorescence emission recorded in these species (Fig. 5A).

It was suggested that additional chromophores may contribute to low-energy absorption in PSI–LHCI subunits. For instance, the extra Chl *a*615 (also known as *a*617) was assigned to the Lhca4 subunit of land plants based on structural homology with the LHCII monomer [179]. Its presence has been experimentally confirmed through structural analysis of the PSI–LHCI SC of *P. sativum* (PDB 7DKZ) [22], *Z. mays* (PDB 5ZJI) [180] and *F. albivenis* (PDB 8WGH) [100]. However, recent mutational studies conducted *in vivo* have excluded its direct involvement in the formation of RFs [106].

Some reports have suggested that Chl *b* may also contribute to the stabilization of RFs in Lhca4, although the exact identity of the pigments involved is still unknown [90,93,181].

As previously mentioned, some eukaryotic microalgae display different types of PSII outer antennae that enable FR light absorption. For instance, the freshwater species *P. crispa* (Trebouxiophyceae) possesses a ring-shaped endecameric LHCII system consisting of four-helix Pc-frLHC monomers in addition to the canonical trimeric arrangement of three-helix LHCs [182,183]. These circular complexes display a red-shifted absorption around 710 nm originating from the strongly interacting Chl *a*603–*a*609 pair housed inside the Pc-frLHC subunits, which is responsible for a large excitation-induced permanent dipole moment between the two Chls with a pronounced CT character. In addition, Chl *a*609 appears to be excitonically coupled with the neighboring Chl

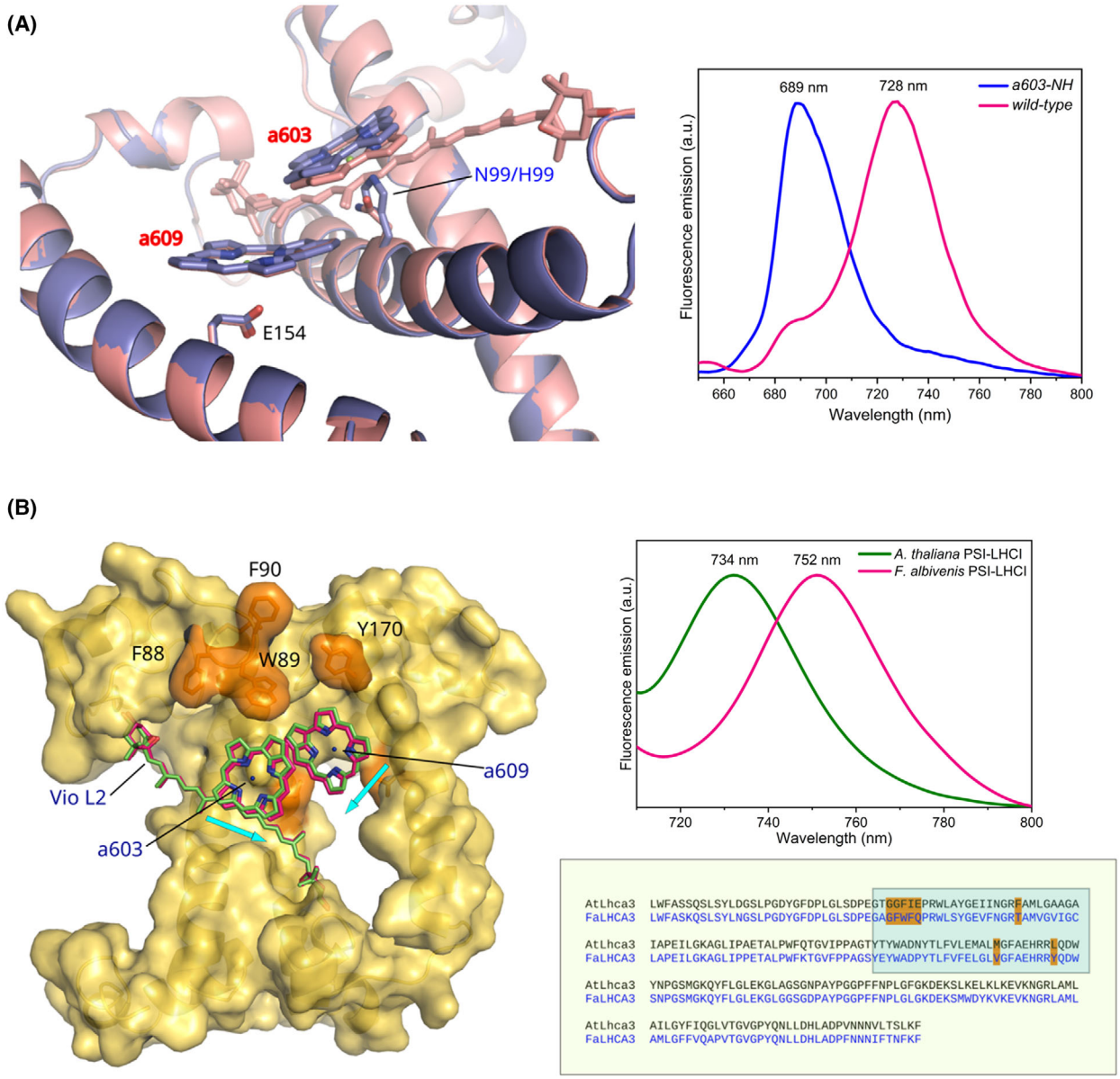

Fig. 5. Structural determinants of low-energy absorption in the Lhca3 and Lhca4 subunits of the PSI–LHCI supercomplex of higher plants. (A) Position of Chls *a*603 and *a*609 in the wild type (salmon; PDB 9GBI) and in the Asn (N)99-His (H) mutant (blue; PDB 9GC2) Lhca4 subunit of the *A. thaliana* PSI–LHCI supercomplex. The effect of the mutation on fluorescence emission at 77 K of isolated Lhca heterodimers is shown in the right box and is based on [106]. (B) The presence of a group of bulky hydrophobic residues in the vicinity of the Chl pair *a*603–*a*609 (red) in Lhca3 of *Fittonia albivenis* (PDB 8WGH [100]) causes a subtle displacement of the chlorine rings compared to *A. thaliana* (green), causing a red-shifted fluorescence emission (right). The lower box displays the sequence alignment between the Lhca3 isoforms of *A. thaliana* and *F. albivenis*, highlighting the short hydrophobic amino acid stretch and three residues that potentially contribute to the strongly red-shifted fluorescence emission (highlighted in orange inside the blue box). Cyan arrows indicate the displacement of chromophores due to differences in the local protein environment. This figure was created using The PyMOL software/ Molecular Graphics System, Version 3.0 Schrödinger, LLC. The multiple sequence alignment was performed using the Clustal Omega (EMBL-EBI) [175] using the Lhca3 amino acid sequences retrieved from PDB 8WGH (*F. albivenis*) [100] and PDB 9GBI (*A. thaliana*).

*a*708, possibly forming a Chl trimer, which provides the structural basis for FR light absorption. Finally, more subtle alterations of the protein environment appear to enable FR light absorption by the only Chl *a*-based LHC system in some eustigmatophytes [184,185].

Bioengineering low-energy absorption in plants

Rational genetic engineering has the potential to significantly accelerate the development of elite crop cultivars by enhancing their resource-use efficiency [186]. Among various traits, photosynthesis is an emerging target for crop improvement, with multiple strategies proposed to increase the efficiency of sunlight-to-biomass conversion (for detailed reviews see [187–191]). Bioengineering the absorption of low-energy photons in plants can expand the light-harvesting capacity of leaves, thereby boosting photosynthesis under light conditions enriched with longer wavelengths, for example beneath dense canopies [192,193]. Ideally, a "smartly designed" crop canopy should facilitate the uniform distribution of wavelengths throughout its vertical profile [194] (Fig. 6). This could be achieved, for example, by regulating the leaf angle, or by lowering leaf Chl content to decrease the canopy optical density [195–197]. Alternatively, the light-harvesting apparatus of shaded foliage could be tuned to efficiently utilize the available light spectrum, particularly by maximizing the interception of photons in the red-most PAR region [196].

Independent studies have suggested that, by fully harnessing the absorption of the 700–750 nm range, energy conversion in crops could be enhanced between 19 and 26% [192,193,198], representing a significant improvement compared to the estimated 4–6% efficiency observed in most crop species [199]. This bioengineering concept is eliciting great interest and could be achieved through a combination of approaches (Fig. 6).

One strategy involves incorporating red-shifted prokaryotic Chl types (Chl *d* and *f*) into eukaryotic LHC complexes, to enable excitation by photons with lower energy than those typically absorbed by Chl *a* and *b* (for a dedicated review, see [72]). The feasibility of this approach has been demonstrated *in vitro*, where Chl *d* and *f* could be incorporated into the plant Lhca4 protein, causing a pronounced red-shift without compromising its functions and structural integrity [200]. Moreover, Chl *d* has been successfully integrated into the plant LHCII complex *in vitro*, producing an ~25 nm absorption red-shift while maintaining the native protein architecture, EET and energy quenching [201,202]. However, the implementation of heterologous Chl biosynthesis in plants remains unreported and faces at least three major challenges: (i) the factor(s) required for Chl *d* synthesis are yet to be identified [203,204], (ii) the *in vivo* incorporation of non-native Chl types into eukaryotic LHCs may be suboptimal [205] and (iii) inserting low-energy pigments into Chl *a*-dominated eukaryotic LHCs could create energy traps, thereby slowing EET and energy trapping, especially in the PSII RC [206].

A second strategy, discussed in the next paragraph, aims at broadening the absorption capacity of light-harvesting systems by modifying the native pigment–pigment and pigment–protein interactions through engineering of the protein scaffold to create novel spectral properties of LHCs.

Spectral tuning of LHCs through novel pigment–protein interactions

The spectral properties of LHCs can be modified to enhance FR light absorption via substitutions of key chlorophyll-binding residues and/or altering the local protein microenvironment. Such changes influence the spatial arrangement (distance and orientation) of pigment pairs, thereby affecting pigment–pigment and pigment–protein interactions. This, in turn, shifts the balance between EC and CT states. Since excitonic interactions are highly sensitive to the local environment, even subtle structural modifications of the protein scaffold can reshape pigment geometry, leading to notable changes in the protein spectral responses [207].

LHC proteins exhibit a highly conserved three-dimensional architecture characterized by three transmembrane helices interconnected by amphiphilic loops [208]. In plant LHCs, at least six conserved residues are involved in Chl coordination, along with other key residues that shape the local protein microenvironment. Several of these residues are thus promising targets for mutagenesis [41].

The first proof-of-concept study reporting the *in vivo* engineering of these interactions was performed in the photosynthetic purple bacterium *Rhodobacter sphaeroides*. This work established a direct correlation between the absorbance properties of bacteriochlorophyll *a* and two coordinating tyrosine residues (Tyr44 and Tyr45) in the α subunit of the peripheral light-harvesting complex LH2 [176,209]. The single and double substitution of Tyr44 with Phe and Tyr45 with Leu caused blue-shifts of 11 and 24 nm, respectively. The same rationale was employed *in vitro* with the plant subunits rLhca3 and rLhca4, leading to the identification of the Asn ligand of Chl *a*603 as the structural determinant responsible for the red-shifted emission [95]. This approach was subsequently tested in *A. thaliana* by replacing the Asn coordinating Chl *a*603 in the Lhca4, producing a 2–3 nm blue-shift of

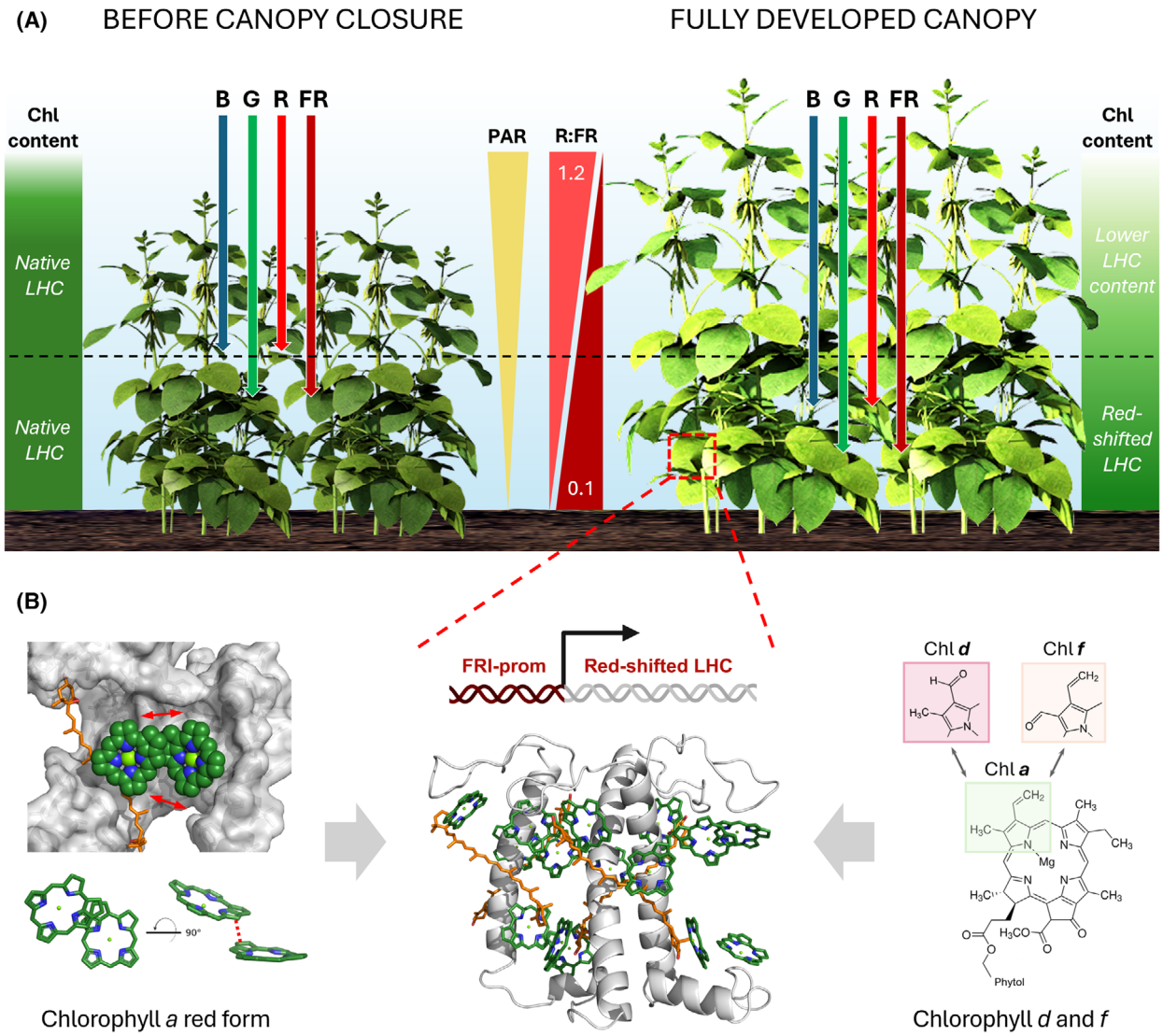

Fig. 6. Proposed 'smart canopy', engineered to optimize the efficiency of FR light use in dense crop monocultures. Panel (A) illustrates two stages of canopy growth. Left: Before canopy closure, the light-harvesting apparatus consists of a native complement of LHC proteins, and leaf chlorophyll (Chl) content is homogeneous across leaf layers. In this configuration, the top leaves act as a filter for incoming photosynthetically active radiation (PAR), limiting the penetration of blue (B) and red (R) photons. Therefore, the lower leaf layers receive predominantly green (G) and far-red (FR) wavelengths, as reflected by a markedly reduced R:FR ratio. Right: In a fully developed canopy, a gradual reduction in Chl content from the top to the bottom foliage should promote a more uniform light distribution within the canopy. The predominantly FR light environment in the lower layers could act as a trigger to induce the expression of red-shifted LHCs, to enable efficient utilization of the available spectrum. Panel (B): A feasible strategy to enhance low-energy absorption involves using FR-inducible (FRI) promoters to drive expression in the lower leaf layers of red-shifted LHCs incorporating chlorophyll *d* and *f* or carrying structural modifications such as novel pigment–protein and pigment–pigment interactions. Centre: conserved structure of an LHC protein (Lhca4; PDB: 9GBI) with bound chlorophylls (green) and carotenoids (orange), showing their organization within the scaffold (gray). Left: Close-up view of inter-pigment interactions within LHCs, highlighting Chl *a* molecules, their coupling, and the geometry influenced by the binding site and local protein environment. Right: Chemical structures of Chl *a*, *d*, and *f*. The structural models in this figure was created using The PyMOL Molecular Graphics System, Version 3.0 Schrödinger, LLC.

the emission peak at 77 K of the isolated PSI–LHCI SC [172]. Instead, the double substitution of Asn with His in both Lhca3 and Lhca4 resulted in a greater blue-shift, around 13 nm, in the isolated PSI–LHCI SC and a 39 nm shift in the isolated LHCI heterodimers [106]. Intriguingly, replacing a Glu residue located in the transmembrane helix with Gln slightly enhanced the native red-shift [43,172].

A similar *in vivo* strategy was used with the PSII monomeric antenna protein Lhcb4 (CP29) in *A. thaliana*, in which the His residue coordinating Chl *a*603 was substituted with Asn (His111Asn) [173,174]. Despite the marked structural similarity between Lhcb4, Lhca3, and Lhca4, this mutation resulted in an ~14 nm red-shift in the 77 K fluorescence difference spectra compared to the wild-type, which is substantially lower than the ~39 and 44 nm shifts observed in Lhca3 and Lhca4, respectively [95,173–174]. Furthermore, the calculated difference in absorption spectra (Lhcb4 wild-type minus His/Asn mutant) revealed a conserved signal in the Q_x region, with a negative peak at 676 nm and a positive peak at 686 nm [173]. This 10 nm shift was attributed to enhanced EC between the Chl pair *a*603–*a*609. Moreover, the mutant Lhcb4 isoform displayed a shorter fluorescence lifetime and a reduced formation of carotenoid triplet states, indicating an increased quenching capacity stemming from stronger pigment–pigment interactions [173]. Altogether, these results indicate that subtle modifications within the pigment-binding pockets, either caused by altering the identity of the Chl ligand or the surrounding and distal residues, can lower the pigment energy levels and create new spectral features. However, it is important to recognize the multifactorial nature of the spectral features of LHCs, which are shaped by the presence of multiple interacting Chl and carotenoid molecules [210]. Furthermore, some Chls are coordinated by water molecules, lipids, or backbone atoms, making them less amenable to modifications via side-chain substitutions. Instead, certain mutations may destabilize protein folding and/or interfere with pigment incorporation, limiting the accumulation of the holoprotein [174]. Finally, introducing low-energy states into LHCs could have pleiotropic effects on the overall light-harvesting process, potentially impacting light-use efficiency and, thus, plant growth.

To better understand and predict the effects of mutations, researchers have employed molecular dynamics simulations and quantum chemical models to study how factors such as local polarity, conformational flexibility, and the dielectric environment influence pigment site energies and EC [211,212]. Building on this foundation, machine learning techniques are increasingly being recognized as powerful tools for predictive bioengineering. For instance, networks trained on excitonic energy transfer dynamics can learn complex structure–function relationships and predict how specific mutations may impact pigment coupling and spectral shifts [213]. This approach has the potential to enable high-throughput *in silico* screening of LHC variants, aiding the identification of promising mutations for experimental validation and accelerating the design of red-shifted or spectrally broadened antenna complexes.

Optimizing canopy light-use efficiency

The photosynthesis-enhancement resulting from broadened light absorption of leaves is expected to translate into crop applications. However, the direct transfer of technologies from a rosette-forming plant such as *A. thaliana* to canopy-forming species is not always straightforward [214–216]. A more effective approach involves engineering photosynthesis at the canopy level. A "smart canopy" concept should include a vertically stratified and self-organizing system in which leaves dynamically adjust their photosynthetic capacity based on the local light environment [187]. The spatial heterogeneity in light quality could be addressed by tuning the leaf absorption properties to match the irradiance spectra at various canopy heights or during different plant developmental stages. For instance, this spectral stratification could be achieved via spatiotemporal control of pigment biosynthesis in leaves and/or by selectively expressing red-shifted LHC isoforms (Fig. 6) [196,217].

Red-shifted light-harvesting systems could be preferentially assembled in the lower foliage, exploiting transcriptional activation by heterologous promoters responding to low R:FR ratio [218], as recently suggested based on simulation of 3D canopy model [198]. Consequently, the identification of FR-light-inducible promoters, such as those belonging to phytochrome-based signaling pathways, is a necessary step toward this goal. These bioengineering strategies might be further supported by modeling approaches that estimate the impact of new leaf phenotypes on overall canopy photosynthetic capacity [217,219–221]. Indeed, the predictive power of functional–structural plant models relies on integrating multiple parameters, such as 3D canopy architecture, internal light distribution, ray-tracing, CO_2 diffusion rates inside leaf tissues, acclimation of photosynthesis to fluctuating light, and allocation of photosynthates between organs. Modeling could also help quantify the trade-offs between metabolic investment and yield gains, thus addressing key barriers to develop optimized crop varieties [222–229].

Too far (red) to be true?

The absorption of FR light in photosynthesis is a dynamic process spanning several orders of magnitude, from ecosystems to the molecular architecture of

photosystems. At present, the term "RFs is used interchangeably to describe a spectroscopic feature (such as a wavelength threshold) or the structural determinant responsible for long-wavelength absorption. However, the exact localization of RFs cannot be reliably determined solely from structural data, making red-shifted bands largely volatile spectroscopic attributes [43,138,140,154,181,230].

The ability to engineer the spectroscopic features of LHCs is expected to prompt a revision of the current definition of RFs, embracing new types of excitonic interactions deriving from rational design approaches [231–234]. Nonetheless, efforts to enhance FR light absorption, such as incorporating heterologous Chl types or modifying the LHC protein matrix, must contend with structural and biophysical constraints, which can impact EET dynamics, charge separation, and other feedback regulatory mechanisms [235–241]. The continuous investigation into the structural and functional properties of LHCs is expected to facilitate the transfer of spectroscopic phenotypes between LHC isoforms. To support this, developing methods to predict excited-state energy levels of FR pigments and assess the effects of tuning interventions is crucial.

A promising approach involves integrating high-resolution structural analyses with quantum mechanical calculations to elucidate how subtle protein modifications can affect FR absorption and excited-state lifetimes, as recently reported for EET pathway analysis in PSII [242]. Finally, the biodiversity of light-harvesting systems represents an immensely valuable resource for translational research and nature-based engineering. Phylogenetic comparative methods coupled with structural–functional investigations could help identify and pinpoint factors responsible for long-wavelength absorption. In particular, the study of organisms adapted to natural, light-limited environments, such as understory or aquatic habitats, could offer insightful models to guide LHC spectral tuning. This interdisciplinary integration will be essential for developing next-generation crops capable of dynamic spectral partitioning across canopy layers, ultimately enhancing productivity.

Acknowledgements

The authors acknowledge the financial support from the Ministry of Education, University and Research (MIUR grant driveALGAE: 2022FXRZBF–PRIN2022) to LD, and from the European Research Council (European Research Council Advanced Grant 101053983-GrInSun) to RB. Open access publishing facilitated by Università degli Studi di Verona, as part of the Wiley - CRUI-CARE agreement. Open access publishing facilitated by Universita degli Studi di Verona, as part of the Wiley - CRUI-CARE agreement.

Author contributions

LD and DM conceived this manuscript. AA, EAC, DM, CB, SC, RC, and ZG conducted the bibliographic review and contributed to the writing. AA, EAC, SC, LD, and ZG prepared the figures. RB supervised the manuscript preparation and edited the final version.

References

1 Croce R and van Amerongen H (2014) Natural strategies for photosynthetic light harvesting. *Nat Chem Biol* **10** (7), 492–501.
2 Bag P (2021) Light harvesting in fluctuating environments: evolution and function of antenna proteins across photosynthetic lineage. *Plants (Basel)* **10** (6),
3 Eberhard S, Finazzi G and Wollman FA (2008) The dynamics of photosynthesis. *Annu Rev Genet* **42**, 463–515.
4 Niinemets U and Valladares F (2004) Photosynthetic acclimation to simultaneous and interacting environmental stresses along natural light gradients: optimality and constraints. *Plant Biol (Stuttg)* **6** (3), 254–268.
5 De Castro F (2000) Light spectral composition in a tropical forest: measurements and model. *Tree Physiol* **20** (1), 49–56.
6 Chelle M, Evers JB, Combes D, Varlet-Grancher C, Vos J and Andrieu B (2007) Simulation of the three-dimensional distribution of the red: far-red ratio within crop canopies. *New Phytol* **176** (1), 223–234.
7 Liu W, Mõttus M, Malenovský Z, Shi S, Alonso L, Atherton J and Porcar-Castell A (2025) An in situ approach for validation of canopy chlorophyll fluorescence radiative transfer models using the full emission spectrum. *Remote Sens Environ* **316**, 114490.
8 Chen G, Chen H, Shi K, Raza MA, Bawa G, Sun X, Pu T, Yong T, Liu W, Liu J *et al.* (2020) Heterogeneous light conditions reduce the assimilate translocation towards maize ears. *Plants* **9** (8), 987.
9 Feng L, Shi K, Liu X, Yang H, Pu T, Wu Y, Yong T, Yang F, Wang X, van Groenigen KJ *et al.* (2024) Optimizing trade-offs between light transmittance and intraspecific competition under varying crop layouts in a maize–soybean strip relay cropping system. *The Crop Journal* **12** (6), 1780–1790.
10 Dreccer MF, Zwart AB, Schmidt R-C, Condon AG, Awasi MA, Grant TJ, Galle A, Bourot S and

Frohberg C (2022) Wheat yield potential can be maximized by increasing red to far-red light conditions at critical developmental stages. *Plant Cell Environ* **45** (9), 2652–2670.
11 Ritchie RJ, Larkum AWD and Ribas I (2018) Could photosynthesis function on Proxima Centauri b? *Int J Astrobiol* **17** (2), 147–176.
12 Malone LA, Qian P, Mayneord GE, Hitchcock A, Farmer DA, Thompson RF, Swainsbury DJK, Ranson NA, Hunter CN and Johnson MP (2019) Cryo-EM structure of the spinach cytochrome b6 f complex at 3.6 Å resolution. *Nature* **575** (7783), 535–539.
13 Fields BA, Bartsch HH, Bartunik HD, Cordes F, Guss JM and Freeman HC (1994) Accuracy and precision in protein crystal structure analysis: two independent refinements of the structure of poplar plastocyanin at 173 K. *Acta Crystallogr D Biol Crystallogr* **50** (Pt 5), 709–730.
14 Binda C, Coda A, Aliverti A, Zanetti G and Mattevi A (1998) Structure of the mutant E92K of [2Fe-2S] ferredoxin I from Spinacia oleracea at 1.7 A resolution. *Acta Crystallogr D Biol Crystallogr* **54** (Pt 6 Pt 2), 1353–1358.
15 Bruns CM and Karplus AP (1995) Refined crystal structure of spinach ferredoxin reductase at 1.7 Å resolution: oxidized, reduced and 2′-phospho-5′-AMP bound states. *J Mol Biol* **247** (1), 125–145.
16 Hahn A, Vonck J, Mills DJ, Meier T and Kühlbrandt W (2018) Structure, mechanism, and regulation of the chloroplast ATP synthase. *Science* **360** (6389),
17 Björn LO, Papageorgiou GC, Blankenship RE and Govindjee (2009) A viewpoint: why chlorophyll a? *Photosynth Res* **99**, 85–98.
18 Nelson N and Ben-Shem A (2004) The complex architecture of oxygenic photosynthesis. *Nat Rev Mol Cell Biol* **5** (12), 971–982.
19 Laisk A, Oja V, Eichelmann H and Dall'Osto L (2014) Action spectra of photosystems II and I and quantum yield of photosynthesis in leaves in State 1. *Biochimica et Biophysica Acta (BBA) - Bioenergetics* **1837** (2), 315–325.
20 Antonaru LA, Rad-Menéndez C, Mbedi S, Sparmann S, Pope M, Oliver T, Wu S, Green DH, Gugger M and Nürnberg DJ (2025) Evolution of far-red light photoacclimation in cyanobacteria. *Curr Biol* **35** (11), 2539–2553.e4.
21 Jensen PE, Bassi R, Boekema EJ, Dekker JP, Jansson S, Leister D, Robinson C and Scheller HV (2007) Structure, function and regulation of plant photosystem I. *Biochim Biophys Acta* **1767** (5), 335–352.
22 Qin X, Suga M, Kuang T and Shen J-R (2015) Structural basis for energy transfer pathways in the plant PSI-LHCI supercomplex. *Science* **348** (6238), 989–995.
23 Mazor Y, Borovikova A, Caspy I and Nelson N (2017) Structure of the plant photosystem I supercomplex at 2.6 Å resolution. *Nat Plants* **3**, 17014.
24 Caspy I and Nelson N (2018) Structure of the plant photosystem I. *Biochem Soc Trans* **46** (2), 285–294.
25 Rivadossi A, Zucchelli G, Garlaschi FM and Jennings RC (1999) The importance of PS I chlorophyll red forms in light-harvesting by leaves. *Photosynth Res* **60** (2), 209–215.
26 Gobets B and van Grondelle R (2001) Energy transfer and trapping in photosystem I. *Biochim Biophys Acta* **1507** (1-3), 80–99.
27 Vasil'ev S and Bruce D (2004) Optimization and Evolution of Light Harvesting in Photosynthesis: The Role of Antenna Chlorophyll Conserved between Photosystem II and Photosystem I. *Plant Cell* **16** (11), 3059–3068.
28 Heckman DS, Geiser DM, Eidell BR, Stauffer RL, Kardos NL and Hedges SB (2001) Molecular evidence for the early colonization of land by fungi and plants. *Science* **293** (5532), 1129–1133.
29 Alboresi A, Caffarri S, Nogue F, Bassi R and Morosinotto T (2008) In silico and biochemical analysis of Physcomitrella patens photosynthetic antenna: identification of subunits which evolved upon land adaptation. *PLoS One* **3** (4), e2033.
30 Rensing SA, Lang D, Zimmer AD, Terry A, Salamov A, Shapiro H, Nishiyama T, Perroud PF, Lindquist EA, Kamisugi Y *et al.* (2008) The Physcomitrella genome reveals evolutionary insights into the conquest of land by plants. *Science* **319** (5859), 64–69.
31 Alboresi A, Gerotto C, Giacometti GM, Bassi R and Morosinotto T (2010) Physcomitrella patens mutants affected on heat dissipation clarify the evolution of photoprotection mechanisms upon land colonization. *Proc Natl Acad Sci* **107** (24), 11128–11133.
32 Gerotto C and Morosinotto T (2013) Evolution of photoprotection mechanisms upon land colonization: evidence of PSBS-dependent NPQ in late Streptophyte algae. *Physiol Plant* **149** (4), 583–598.
33 Servais T, Cascales-Miñana B, Cleal CJ, Gerrienne P, Harper DAT and Neumann M (2019) Revisiting the Great Ordovician diversification of land plants: recent data and perspectives. *Palaeogeogr Palaeoclimatol Palaeoecol* **534**, 109280.
34 Condamine FL, Silvestro D, Koppelhus EB and Antonelli A (2020) The rise of angiosperms pushed conifers to decline during global cooling. *Proc Natl Acad Sci* **117** (46), 28867–28875.
35 Rensing SA (2020) How Plants Conquered Land. *Cell* **181** (5), 964–966.
36 Benton MJ, Wilf P and Sauquet H (2022) The Angiosperm Terrestrial Revolution and the origins of modern biodiversity. *New Phytol* **233** (5), 2017–2035.

37 Gorski C, Riddle R, Toporik H, Da Z, Dobson Z, Williams D and Mazor Y (2022) The structure of the Physcomitrium patens photosystem I reveals a unique Lhca2 paralogue replacing Lhca4. *Nat Plants* **8** (3), 307–316.
38 Kumar P, Kumar P, Verma V, Irfan M, Sharma R and Bhargava B (2023) How plants conquered land: evolution of terrestrial adaptation. *J Evol Biol* **35** (5), 5–14.
39 Rieseberg TP, Dadras A, Darienko T, Post S, Herrfurth C, Fürst-Jansen JMR, Hohnhorst N, Petroll R, Rensing SA, Pröschold T *et al.* (2025) Time-resolved oxidative signal convergence across the algae–embryophyte divide. *Nat Commun* **16** (1), 1780.
40 Perez-Boerema A, Engel BD and Wietrzynski W (2024) Evolution of thylakoid structural diversity. *Annu Rev Cell Dev Biol* **40** (2024), 169–193.
41 Iwai M, Patel-Tupper D and Niyogi KK (2024) Structural diversity in eukaryotic photosynthetic light harvesting. *Annu Rev Plant Biol* **75**, 119–152.
42 Croce R and van Amerongen H (2020) Light harvesting in oxygenic photosynthesis: structural biology meets spectroscopy. *Science* **369** (6506),
43 Wientjes E, Roest G and Croce R (2012) From red to blue to far-red in Lhca4: how does the protein modulate the spectral properties of the pigments? *Biochimica et Biophysica Acta (BBA) - Bioenergetics* **1817** (5), 711–717.
44 Pedersen O, Colmer TD and Sand-Jensen K (2013) Underwater photosynthesis of submerged plants – recent advances and methods. *Front Plant Sci* **4**,
45 Wolf BM and Blankenship RE (2019) Far-red light acclimation in diverse oxygenic photosynthetic organisms. *Photosynth Res* **142** (3), 349–359.
46 Fernández-Marín B, Gulías J, Figueroa CM, Iñiguez C, Clemente-Moreno MJ, Nunes-Nesi A, Fernie AR, Cavieres LA, Bravo LA, García-Plazaola JI *et al.* (2020) How do vascular plants perform photosynthesis in extreme environments? An integrative ecophysiological and biochemical story. *Plant J* **101** (4), 979–1000.
47 Arshad R, Saccon F, Bag P, Biswas A, Calvaruso C, Bhatti AF, Grebe S, Mascoli V, Mahbub M, Muzzopappa F *et al.* (2022) A kaleidoscope of photosynthetic antenna proteins and their emerging roles. *Plant Physiol*
48 Lan Y, Song Y, Zhao F, Cao Y, Luo D, Qiao D, Cao Y and Xu H (2023) Phylogenetic, structural and functional evolution of the LHC gene family in plant species. *Int J Mol Sci* **24** (1), 488.
49 Park Y and Runkle ES (2017) Far-red radiation promotes growth of seedlings by increasing leaf expansion and whole-plant net assimilation. *Environ Exp Bot* **136**, 41–49.
50 Tan T, Li S, Fan Y, Wang Z, Ali Raza M, Shafiq I, Wang B, Wu X, Yong T, Wang X *et al.* (2022) Far-red light: a regulator of plant morphology and photosynthetic capacity. *The Crop Journal* **10** (2), 300–309.
51 Taylor CR, van Ieperen W and Harbinson J (2025) Greater than the sum of the parts: revisiting the enhancement effect in photosynthesis using simulated sun- and shade-light. *Plant Cell Environ* **48** (8), 6102–6117.
52 Zhen S and Bugbee B (2020) Substituting far-red for traditionally defined photosynthetic photons results in equal canopy quantum yield for CO2 fixation and increased photon capture during long-term studies: implications for re-defining par. *Front Plant Sci* **11**,
53 Zhen S, van Iersel MW and Bugbee B (2022) Photosynthesis in sun and shade: the surprising importance of far-red photons. *New Phytol* **236** (2), 538–546.
54 Rauser WE (1970) Photosynthesis: a simple demonstration of the Emerson enhancement effect. *Am Biol Teach* **32** (6), 333–336.
55 Zhen S and van Iersel MW (2017) Far-red light is needed for efficient photochemistry and photosynthesis. *J Plant Physiol* **209**, 115–122.
56 Kono M, Kawaguchi H, Mizusawa N, Yamori W, Suzuki Y and Terashima I (2020) Far-red light accelerates photosynthesis in the low-light phases of fluctuating light. *Plant Cell Physiol* **61** (1), 192–202.
57 Zhen S and Bugbee B (2020) Far-red photons have equivalent efficiency to traditional photosynthetic photons: implications for redefining photosynthetically active radiation. *Plant Cell Environ* **43** (5), 1259–1272.
58 Cutolo EA, Caferri R, Guardini Z, Dall'Osto L and Bassi R (2023) Analysis of state 1—state 2 transitions by genome editing and complementation reveals a quenching component independent from the formation of PSI-LHCI-LHCII supercomplex in Arabidopsis thaliana. *Biol Direct* **18** (1), 49.
59 Rantala M, Rantala S and Aro E-M (2020) Composition, phosphorylation and dynamic organization of photosynthetic protein complexes in plant thylakoid membrane. *Photochem Photobiol Sci* **19** (5), 604–619.
60 Nguyen TNP and Sung J (2025) Light spectral-ranged specific metabolisms of plant pigments. *Meta* **15** (1), 1.
61 Hu C, Nawrocki WJ and Croce R (2021) Long-term adaptation of *Arabidopsis thaliana* to far-red light. *Plant Cell Environ* **44** (9), 3002–3014.
62 Pashkovskiy P, Khalilova L, Vereshchagin M, Voronkov A, Ivanova T, Kosobryukhov AA, Allakhverdiev SI, Kreslavski VD and Kuznetsov VV (2023) Impact of varying light spectral compositions on photosynthesis, morphology, chloroplast

ultrastructure, and expression of light-responsive genes in Marchantia polymorpha. *Plant Physiol Biochem* **203**, 108044.
63 Lazzarin M, Dupont K, van Ieperen W, Marcelis LFM and Driever SM (2024) Far-red light effects on plant photosynthesis: from short-term enhancements to long-term effects of artificial solar light. *Ann Bot*
64 Leschevin M, Ksas B, Baltenweck R, Hugueney P, Caffarri S and Havaux M (2024) Photosystem rearrangements, photosynthetic efficiency, and plant growth in far red-enriched light. *Plant J* **120** (6), 2536–2552.
65 Carvalho SD and Folta KM (2014) Environmentally modified organisms – expanding genetic potential with light. *Crit Rev Plant Sci* **33** (6), 486–508.
66 Legris M, Ince YÇ and Fankhauser C (2019) Molecular mechanisms underlying phytochrome-controlled morphogenesis in plants. *Nat Commun* **10** (1), 5219.
67 Küpers JJ, Snoek BL, Oskam L, Pantazopoulou CK, Matton SEA, Reinen E, Liao C-Y, Eggermont EDC, Weekamp H, Biddanda-Devaiah M *et al.* (2023) Local light signaling at the leaf tip drives remote differential petiole growth through auxin-gibberellin dynamics. *Curr Biol* **33** (1), 75–85.e5.
68 Yang C and Li L (2017) Hormonal regulation in shade avoidance. *Front Plant Sci* 8.
69 Jans TB, Mossink L, Wassenaar M, Wientjes E, Driever S, Huber M, Pierik R and de Boer HJ Coupling modelling and experiments to analyse leaf photosynthesis under far-red light. *Plant Cell Environ* n/a(n/a)
70 Legendre R and van Iersel MW (2021) Supplemental far-red light stimulates lettuce growth: disentangling morphological and physiological effects. *Plants* **10** (1), 166.
71 Lauria G, Ceccanti C, Lo Piccolo E, El Horri H, Guidi L, Lawson T and Landi M (2024) "Metabolight": how light spectra shape plant growth, development and metabolism. *Physiol Plant* **176** (6), e14587.
72 Elias E, Oliver TJ and Croce R (2024) Oxygenic photosynthesis in far-red light: strategies and mechanisms. *Annu Rev Phys Chem* **75**, 231–256.
73 Norman JM and Campbell GS (1989) In Canopy structure, in Plant Physiological Ecology: Field methods and instrumentation (Pearcy RW *et al.*, eds), pp. 301–325. Springer Netherlands, Dordrecht.
74 Morris JL, Puttick MN, Clark JW, Edwards D, Kenrick P, Pressel S, Wellman CH, Yang Z, Schneider H and Donoghue PCJ (2018) The timescale of early land plant evolution. *Proc Natl Acad Sci* **115** (10), E2274–E2283.
75 Brelsford CC, Trasser M, Paris T, Hartikainen SM and Robson TM (2022) Understorey light quality affects leaf pigments and leaf phenology in different plant functional types. *Physiol Plant* **174** (3), e13723.
76 Helbach J, Frey J, Messier C, Mörsdorf M and Scherer-Lorenzen M (2022) Light heterogeneity affects understory plant species richness in temperate forests supporting the heterogeneity–diversity hypothesis. *Ecol Evol* **12** (2), e8534.
77 Silvestro D, Cascales-Miñana B, Bacon CD and Antonelli A (2015) Revisiting the origin and diversification of vascular plants through a comprehensive Bayesian analysis of the fossil record. *New Phytol* **207** (2), 425–436.
78 Harrison CJ and Morris JL (2018) The origin and early evolution of vascular plant shoots and leaves. *Philosophical Transactions of the Royal Society B: Biological Sciences* **373** (1739), 20160496.
79 Dilcher DL, Lott TA, Wang X and Wang Q (2004) *CHAPTER 6 - A History of Tree Canopies*. In Forest Canopies (Second Edition) (Lowman MD and Rinker HB, eds), pp. 118–137. Academic Press, San Diego.
80 Qin X, Pi X, Wang W, Han G, Zhu L, Liu M, Cheng L, Shen J-R, Kuang T and Sui S-F (2019) Structure of a green algal photosystem I in complex with a large number of light-harvesting complex I subunits. *Nat Plants* **5** (3), 263–272.
81 Su X, Ma J, Pan X, Zhao X, Chang W, Liu Z, Zhang X and Li M (2019) Antenna arrangement and energy transfer pathways of a green algal photosystem-I–LHCI supercomplex. *Nat Plants* **5** (3), 273–281.
82 Yan Q, Zhao L, Wang W, Pi X, Han G, Wang J, Cheng L, He Y, Kuang T, Qin X *et al.* (2021) Antenna arrangement and energy-transfer pathways of PSI–LHCI from the moss Physcomitrella patens. *Cell discovery* **7** (1), 10.
83 Ben-Shem A, Frolow F and Nelson N (2004) Evolution of photosystem I – from symmetry through pseudosymmetry to asymmetry. *FEBS Lett* **564** (3), 274–280.
84 Croce R and Van Amerongen H (2013) Light-harvesting in photosystem I. *Photosynth Res* **116**, 153–166.
85 Rolo D, Schöttler MA, Sandoval-Ibáñez O and Bock R (2024) Structure, function, and assembly of PSI in thylakoid membranes of vascular plants. *Plant Cell* **36** (10), 4080–4108.
86 Wientjes E, van Stokkum IH, van Amerongen H and Croce R (2011) Excitation-energy transfer dynamics of higher plant photosystem I light-harvesting complexes. *Biophys J* **100** (5), 1372–1380.
87 Wientjes E, van Stokkum IH, van Amerongen H and Croce R (2011) The role of the individual Lhcas in photosystem I excitation energy trapping. *Biophys J* **101** (3), 745–754.
88 Schmid VH, Cammarata KV, Bruns BU and Schmidt GW (1997) In vitro reconstitution of the photosystem

I light-harvesting complex LHCI-730: heterodimerization is required for antenna pigment organization. *Proc Natl Acad Sci USA* **94** (14), 7667–7672.
89 Morosinotto T, Baronio R and Bassi R (2002) Dynamics of chromophore binding to Lhc proteins in vivo and in vitro during operation of the xanthophyll cycle. *J Biol Chem* **277** (40), 36913–36920.
90 Schmid VHR, Potthast S, Wiener M, Bergauer V, Paulsen H and Storf S (2002) Pigment binding of photosystem I light-harvesting proteins*. *J Biol Chem* **277** (40), 37307–37314.
91 Castelletti S, Morosinotto T, Robert B, Caffarri S, Bassi R and Croce R (2003) Recombinant Lhca2 and Lhca3 subunits of the photosystem I antenna system. *Biochemistry* **42** (14), 4226–4234.
92 Croce R, Chojnicka A, Morosinotto T, Ihalainen JA, van Mourik F, Dekker JP, Bassi R and van Grondelle R (2007) The low-energy forms of photosystem I light-harvesting complexes: spectroscopic properties and pigment-pigment interaction characteristics. *Biophys J* **93** (7), 2418–2428.
93 Croce R, Morosinotto T, Castelletti S, Breton J and Bassi R (2002) The Lhca antenna complexes of higher plants photosystem I. *Biochim Biophys Acta* **1556** (1), 29–40.
94 Wientjes E and Croce R (2011) The light-harvesting complexes of higher-plant Photosystem I: Lhca1/4 and Lhca2/3 form two red-emitting heterodimers. *Biochem J* **433** (3), 477–485.
95 Morosinotto T, Breton J, Bassi R and Croce R (2003) The nature of a chlorophyll ligand in Lhca proteins determines the far red fluorescence emission typical of photosystem I. *J Biol Chem* **278** (49), 49223–49229.
96 Klimmek F, Ganeteg U, Ihalainen JA, van Roon H, Jensen PE, Scheller HV, Dekker JP and Jansson S (2005) Structure of the higher plant light harvesting complex I: in vivo characterization and structural interdependence of the Lhca proteins. *Biochemistry* **44** (8), 3065–3073.
97 Wientjes E, Oostergetel GT, Jansson S, Boekema EJ and Croce R (2009) The role of Lhca complexes in the supramolecular organization of higher plant photosystem I. *J Biol Chem* **284** (12), 7803–7810.
98 Chukhutsina VU, Liu X, Xu P and Croce R (2020) Light-harvesting complex II is an antenna of photosystem I in dark-adapted plants. *Nat Plants* **6** (7), 860–868.
99 Bos PR, Schiphorst C, Kercher I, Buis S, de Jong D, Vunderink I and Wientjes E (2023) Spectral diversity of photosystem I from flowering plants. *Photosynth Res* **155** (1), 35–47.
100 Li X, Huang G, Zhu L, Hao C, Sui SF and Qin X (2024) Structure of the red-shifted Fittonia albivenis photosystem I. *Nat Commun* **15** (1), 6325.
101 Morosinotto T, Mozzo M, Bassi R and Croce R (2005) Pigment-pigment interactions in Lhca4 antenna complex of higher plants photosystem I*. *J Biol Chem* **280** (21), 20612–20619.
102 Caffarri S, Tibiletti T, Jennings RC and Santabarbara S (2014) A comparison between plant photosystem I and photosystem II architecture and functioning. *Curr Protein Pept Sci* **15** (4), 296–331.
103 Croce, R. and R. Bassi, The light-harvesting complex of photosystem I: pigment composition and stoichiometry. In Photosynthesis: Mechanisms and Effects: Volume I–V: Proceedings of the XIth International Congress on Photosynthesis, Budapest, Hungary, August 17–22, 1998, G. Garab, Editor. 1998, Springer Netherlands: Dordrecht. p. 421-424.
104 Huang Z, Shen L, Wang W, Mao Z, Yi X, Kuang T, Shen J-R, Zhang X and Han G (2021) Structure of photosystem I-LHCI-LHCII from the green alga Chlamydomonas reinhardtii in State 2. *Nat Commun* **12** (1), 1100.
105 Karapetyan NV, Dorra D, Schweitzer G, Bezsmertnaya IN and Holzwarth AR (1997) Fluorescence spectroscopy of the longwave chlorophylls in trimeric and monomeric photosystem I core complexes from the cyanobacterium Spirulina platensis. *Biochemistry* **36** (45), 13830–13837.
106 Capaldi S, Guardini Z, Montepietra D, Pagliuca VF, Amelii A, Betti E, John C, Pedraza-González L, Cupellini L, Mennucci B *et al.* (2025) Structural determinants for red-shifted absorption in higher-plants Photosystem I. *New Phytol* doi: 10.1111/nph.70562
107 Charras Q, Rey P, Guillemain D, Dourguin F, Laganier H, Peschoux S, Molinié R, Ismaël M, Caffarri S, Rayon C *et al.* (2024) An efficient protocol for extracting thylakoid membranes and total leaf proteins from Posidonia oceanica and other polyphenol-rich plants. *Plant Methods* **20** (1), 38.
108 Mobley CD (1994) Light and water: radiative transfer in natural waters. (No Title).
109 Kirk JTO (2010) Light and Photosynthesis in Aquatic Ecosystems. 3rd edn. Cambridge University Press, Cambridge.
110 Cunningham A, Ramage L and McKee D (2013) Relationships between inherent optical properties and the depth of penetration of solar radiation in optically complex coastal waters. *J Geophys Res Oceans* **118** (5), 2310–2317.
111 Shibata Y, Mohamed A, Taniyama K, Kanatani K, Kosugi M and Fukumura H (2018) Red shift in the spectrum of a chlorophyll species is essential for the drought-induced dissipation of excess light energy in a poikilohydric moss. *Bryum argenteum Photosynthesis Research* **136** (2), 229–243.
112 Iwai M, Grob P, Iavarone AT, Nogales E and Niyogi KK (2018) A unique supramolecular organization of

photosystem I in the moss *Physcomitrella patens*. *Nat Plants* **4** (11), 904–909.
113 Pinnola A and Bassi R (2018) Molecular mechanisms involved in plant photoprotection. *Biochem Soc Trans* **46** (2), 467–482.
114 Sun H, Shang H, Pan X and Li M (2023) Lhcb9-dependent photosystem I structure in moss reveals evolutionary adaptation to changing light conditions during aquatic-terrestrial transition. *bioRxiv* 2023.01.18.524345.
115 Zhang S, Tang K, Yan Q, Li X, Shen L, Wang W, He YK, Kuang T, Han G, Shen JR *et al.* (2023) Structural insights into a unique PSI-LHCI-LHCII-Lhcb9 supercomplex from moss *Physcomitrium patens*. *Nat Plants* **9** (5), 832–846.
116 Alboresi A, Gerotto C, Cazzaniga S, Bassi R and Morosinotto T (2011) A red-shifted antenna protein associated with photosystem II in Physcomitrella patens. *J Biol Chem* **286** (33), 28978–28987.
117 Mozzo M, Mantelli M, Passarini F, Caffarri S, Croce R and Bassi R (2010) Functional analysis of photosystem I light-harvesting complexes (Lhca) gene products of Chlamydomonas reinhardtii. *Biochimica et Biophysica Acta (BBA) -Bioenergetics* **1797** (2), 212–221.
118 Ishii A, Shan J, Sheng X, Kim E, Watanabe A, Yokono M, Noda C, Song C, Murata K, Liu Z *et al.* (2023) The photosystem I supercomplex from a primordial green alga Ostreococcus tauri harbors three light-harvesting complex trimers. *elife* **12**, e84488.
119 Bednarczyk D, Dym O, Prabahar V, Peleg Y, Pike DH and Noy D (2016) Fine Tuning of Chlorophyll Spectra by Protein-Induced Ring Deformation. *Angew Chem Int Ed* **55** (24), 6901–6905.
120 Litvín R, Bína D, Herbstová M, Pazderník M, Kotabová E, Gardian Z, Trtílek M, Prášil O and Vácha F (2019) Red-shifted light-harvesting system of freshwater eukaryotic alga *Trachydiscus minutus* (Eustigmatophyta, Stramenopila). *Photosynth Res* **142** (2), 137–151.
121 Agostini A, Bína D, Barcytė D, Bortolus M, Eliáš M, Carbonera D and Litvín R (2024) Origin of the far-red absorbance in eustigmatophyte algae red-shifted Violaxanthin-Chlorophyll Protein. *bioRxiv* 2024.04.27.591434.
122 Agostini A, Bína D, Barcytė D, Bortolus M, Eliáš M, Carbonera D and Litvín R (2024) Eustigmatophyte model of red-shifted chlorophyll a absorption in light-harvesting complexes. *Communications Biology* **7** (1), 1406.
123 Kosugi M, Ozawa S-I, Takahashi Y, Kamei Y, Itoh S, Kudoh S, Kashino Y and Koike H (2020) Red-shifted chlorophyll a bands allow uphill energy transfer to photosystem II reaction centers in an aerial green alga, Prasiola crispa, harvested in Antarctica. *Biochimica et Biophysica Acta (BBA) - Bioenergetics* **1861** (2), 148139.
124 Kosugi M, Ohtani S, Hara K, Toyoda A, Nishide H, Ozawa S-I, Takahashi Y, Kashino Y, Kudoh S, Koike H *et al.* (2024) Characterization of the far-red light absorbing light-harvesting chlorophyll a/b binding complex, a derivative of the distinctive Lhca gene family in green algae. *Front Plant Sci* 15.
125 Miranda-Astudillo H, Arshad R, de Luna FV, Aguilar-Gonzalez Z, Forêt H, Feller T, Gervasi A, Nawrocki W, Counson C, Morsomme P *et al.* (2025) A unique LHCE light-harvesting protein family is involved in photosystem I and II far-red absorption in *Euglena gracilis*. *bioRxiv* 2025.05.07.652572.
126 Kotabová E, Jarešová J, Kaňa R, Sobotka R, Bína D and Prášil O (2014) Novel type of red-shifted chlorophyll a antenna complex from *Chromera velia*. I. physiological relevance and functional connection to photosystems. *Biochimica et Biophysica Acta (BBA) - Bioenergetics* **1837** (6), 734–743.
127 Wilhelm C and Jakob T (2006) Uphill energy transfer from long-wavelength absorbing chlorophylls to PS II in *Ostreobium* sp. is functional in carbon assimilation. *Photosynth Res* **87** (3), 323–329.
128 Herbstová M, Bína D, Kaňa R, Vácha F and Litvín R (2017) Red-light phenotype in a marine diatom involves a specialized oligomeric red-shifted antenna and altered cell morphology. *Sci Rep* **7** (1), 11976.
129 Bína D, Durchan M, Kuznetsova V, Vácha F, Litvín R and Polívka T (2019) Energy transfer dynamics in a red-shifted violaxanthin-chlorophyll a light-harvesting complex. *Biochim Biophys Acta Bioenerg* **1860** (2), 111–120.
130 Bricker WP, Shenai PM, Ghosh A, Liu Z, Enriquez MG, Lambrev PH, Tan HS, Lo CS, Tretiak S, Fernandez-Alberti S *et al.* (2015) Non-radiative relaxation of photoexcited chlorophylls: theoretical and experimental study. *Sci Rep* **5**, 13625.
131 Gouterman M, Wagnière GH and Snyder LC (1963) Spectra of porphyrins: Part II. Four orbital model. *J Mol Spectrosc* **11** (1), 108–127.
132 Weiss C (1972) The pi electron structure and absorption spectra of chlorophylls in solution. *J Mol Spectrosc* **44** (1), 37–80.
133 Arnold DW, Bradforth S, Kitsopoulos T and Neumark DM (1991) Vibrationally resolved spectra of C2–C11 by anion photoelectron spectroscopy. *J Chem Phys* **95** (12), 8753–8764.
134 Saito K, Mitsuhashi K and Ishikita H (2020) Dependence of the chlorophyll wavelength on the orientation of a charged group: why does the accessory chlorophyll have a low site energy in photosystem II? *J Photochem Photobiol A Chem* **402**, 112799.

135 Dall'Osto L, Bassi R and Ruban A (2014) In Photoprotective Mechanisms: Carotenoids, in Plastid Biology (Theg SM and Wollman F-A, eds), pp. 393–435. Springer New York, New York, NY.
136 Cinque G, Croce R, Holzwarth A and Bassi R (2000) Energy transfer among cp29 chlorophylls: calculated Förster rates and experimental transient absorption at room temperature. *Biophys J* **79** (4), 1706–1717.
137 Seely GR (1966) The structure and chemistry of functional groups.
138 Ihalainen JA, Rätsep M, Jensen PE, Scheller HV, Croce R, Bassi R, Korppi-Tommola JEI and Freiberg A (2003) Red spectral forms of chlorophylls in green plant Psi– a site-selective and high-pressure spectroscopy study. *J Phys Chem B* **107** (34), 9086–9093.
139 Karapetyan, N.V., E. Schlodder, R. van Grondelle, and J.P. Dekker, The long wavelength chlorophylls of photosystem I, in photosystem I: the light-driven plastocyanin:ferredoxin oxidoreductase, J.H. Golbeck, Editor. 2006, Springer Netherlands: Dordrecht. p. 177-192.
140 Sláma V, Cupellini L, Mascoli V, Liguori N, Croce R and Mennucci B (2023) Origin of Low-Lying Red States in the Lhca4 Light-Harvesting Complex of Photosystem I. *The Journal of Physical Chemistry Letters* **14** (37), 8345–8352.
141 Cignoni E, Cupellini L and Mennucci B (2022) A fast method for electronic couplings in embedded multichromophoric systems. *J Phys Condens Matter* **34** (30), 304004.
142 Hsu C-P, You Z-Q and Chen H-C (2008) Characterization of the short-range couplings in excitation energy transfer. *J Phys Chem C* **112** (4), 1204–1212.
143 Hsu C-P (2009) The electronic couplings in electron transfer and excitation energy transfer. *Acc Chem Res* **42** (4), 509–518.
144 You Z-Q and Hsu C-P (2014) Theory and calculation for the electronic coupling in excitation energy transfer. *Int J Quantum Chem* **114** (2), 102–115.
145 Liguori N, Periole X, Marrink SJ and Croce R (2015) From light-harvesting to photoprotection: structural basis of the dynamic switch of the major antenna complex of plants (LHCII). *Sci Rep* **5** (1), 15661.
146 Zhou P and Swain S (1997) Quantum interference in resonance fluorescence for a driven V atom. *Phys Rev A* **56** (4), 3011–3021.
147 Palacios MA, Frese RN, Gradinaru CC, van Stokkum IH, Premvardhan LL, Horton P, Ruban AV, van Grondelle R and van Amerongen H (2003) Stark spectroscopy of the light-harvesting complex II in different oligomerisation states. *Biochim Biophys Acta* **1605** (1-3), 83–95.
148 Golub M, Rusevich L, Irrgang K-D and Pieper J (2018) Rigid versus flexible protein matrix: light-harvesting complex II exhibits a temperature-dependent phonon spectral density. *J Phys Chem B* **122** (28), 7111–7121.
149 van Amerongen H and van Grondelle R (2001) Understanding the energy transfer function of LHCII, the major light-harvesting complex of green plants. *J Phys Chem B* **105** (3), 604–617.
150 van Amerongen H and van Grondelle R (2000) Photosynthetic Excitons. World Scientific.
151 Novoderezhkin VI, Palacios MA, van Amerongen H and van Grondelle R (2004) Energy-transfer dynamics in the LHCII complex of higher plants: modified Redfield approach. *J Phys Chem B* **108** (29), 10363–10375.
152 Vaitekonis S, Trinkunas G and Valkunas L (2005) Red chlorophylls in the exciton model of photosystem I. *Photosynth Res* **86** (1), 185–201.
153 Zucchelli G, Morosinotto T, Garlaschi FM, Bassi R and Jennings RC (2005) The low energy emitting states of the Lhca4 subunit of higher plant photosystem I. *FEBS Lett* **579** (10), 2071–2076.
154 Romero E, Mozzo M, van Stokkum IHM, Dekker JP, van Grondelle R and Croce R (2009) The origin of the low-energy form of photosystem I light-harvesting complex Lhca4: mixing of the lowest exciton with a charge-transfer state. *Biophys J* **96** (5), L35–L37.
155 Novoderezhkin VI, Croce R and van Grondelle R (2018) Dynamics of the mixed exciton and charge-transfer states in light-harvesting complex Lhca4: Hierarchical equation approach. *Biochimica et Biophysica Acta (BBA) - Bioenergetics* **1859** (9), 655–665.
156 Pan X, Cao P, Su X, Liu Z and Li M (2020) Structural analysis and comparison of light-harvesting complexes I and II. *Biochim Biophys Acta Bioenerg* **1861** (4), 148038.
157 Jennings RC, Zucchelli G, Croce R and Garlaschi FM (2003) The photochemical trapping rate from red spectral states in PSI–LHCI is determined by thermal activation of energy transfer to bulk chlorophylls. *Biochimica et Biophysica Acta (BBA) -Bioenergetics* **1557**, 91–98.
158 Russo M, Casazza AP, Cerullo G, Santabarbara S and Maiuri M (2021) Direct evidence for excitation energy transfer limitations imposed by low-energy chlorophylls in photosystem I-light harvesting complex I of land plants. *J Phys Chem B* **125** (14), 3566–3573.
159 Engelmann E, Zucchelli G, Casazza AP, Brogioli D, Garlaschi FM and Jennings RC (2006) Influence of the photosystem I-light harvesting complex I antenna domains on fluorescence decay. *Biochemistry* **45** (22), 6947–6955.

160 Slavov C, Ballottari M, Morosinotto T, Bassi R and Holzwarth AR (2008) Trap-limited charge separation kinetics in higher plant photosystem I complexes. *Biophys J* **94** (9), 3601–3612.
161 Bellingeri M, Montepietra D, Cassi D and Scotognella F (2021) The robustness of the photosynthetic system I energy transfer complex network to targeted node attack and random node failure. *Journal of Complex Networks* **10** (1),
162 Montepietra D, Bellingeri M, Ross AM, Scotognella F and Cassi D (2020) Modelling photosystem I as a complex interacting network. *J R Soc Interface* **17** (172), 20200813.
163 Novoderezhkin VI and Croce R (2023) The location of the low-energy states in Lhca1 favors excitation energy transfer to the core in the plant PSI-LHCI supercomplex. *Photosynth Res* **156** (1), 59–74.
164 Novoderezhkin V, Marin A and van Grondelle R (2011) Intra- and inter-monomeric transfers in the light harvesting LHCII complex: the Redfield–Förster picture. *Phys Chem Chem Phys* **13** (38), 17093–17103.
165 Novoderezhkin VI, Palacios MA, van Amerongen H and van Grondelle R (2005) Excitation dynamics in the LHCII complex of higher plants: modeling based on the 2.72 Angstrom crystal structure. *J Phys Chem B* **109** (20), 10493–10504.
166 Bennett DI, Amarnath K and Fleming GR (2013) A structure-based model of energy transfer reveals the principles of light harvesting in photosystem II supercomplexes. *J Am Chem Soc* **135** (24), 9164–9173.
167 Kreisbeck C and Aspuru-Guzik A (2016) Efficiency of energy funneling in the photosystem II supercomplex of higher plants. *Chem Sci* **7** (7), 4174–4183.
168 Pan X, Liu Z, Li M and Chang W (2013) Architecture and function of plant light-harvesting complexes II. *Curr Opin Struct Biol* **23** (4), 515–525.
169 Saraceno P, Sardar S, Caferri R, Camargo FVA, Dall'Osto L, D'Andrea C, Bassi R, Cupellini L, Cerullo G and Mennucci B (2024) Probing the effect of mutations on light harvesting in CP29 by transient absorption and first-principles simulations. *J Phys Chem Lett* **15** (24), 6398–6408.
170 Müh F, Madjet ME-A and Renger T (2010) Structure-based identification of energy sinks in plant light-harvesting complex II. *J Phys Chem B* **114** (42), 13517–13535.
171 Shibata Y, Nishi S, Kawakami K, Shen J-R and Renger T (2013) Photosystem II does not possess a simple excitation energy funnel: time-resolved fluorescence spectroscopy meets theory. *J Am Chem Soc* **135** (18), 6903–6914.
172 Li X, Zhu L, Song J, Wang W, Kuang T, Yang G, Hao C and Qin X (2023) LHCA4 residues surrounding red chlorophylls allow for fine-tuning of the spectral region for photosynthesis in Arabidopsis thaliana. *Front Plant Sci* **13**,
173 Sardar S, Caferri R, Camargo FVA, Capaldi S, Ghezzi A, Dall'Osto L, D'Andrea C, Cerullo G and Bassi R (2024) Site-directed mutagenesis of the chlorophyll-binding sites modulates excited-state lifetime and chlorophyll-xanthophyll energy transfer in the monomeric light-harvesting complex cp29. *J Phys Chem Lett* **15** (11), 3149–3158.
174 Guardini Z, Bressan M, Caferri R, Bassi R and Dall'Osto L (2020) Identification of a pigment cluster catalysing fast photoprotective quenching response in CP29. *Nat Plants* **6** (3), 303–313.
175 Sievers F, Wilm A, Dineen D, Gibson TJ, Karplus K, Li W, Lopez R, McWilliam H, Remmert M, Söding J *et al.* (2011) Fast, scalable generation of high-quality protein multiple sequence alignments using Clustal Omega. *Mol Syst Biol* **7** (1), 539.
176 Fowler GJ, Visschers RW, Grief GG, van Grondelle R and Hunter CN (1992) Genetically modified photosynthetic antenna complexes with blueshifted absorbance bands. *Nature* **355** (6363), 848–850.
177 Schulte T, Niedzwiedzki DM, Birge RR, Hiller RG, Polívka T, Hofmann E and Frank HA (2009) Identification of a single peridinin sensing Chl-a excitation in reconstituted PCP by crystallography and spectroscopy. *Proc Natl Acad Sci USA* **106** (49), 20764–20769.
178 Cogdell RJ, Gall A and Köhler J (2006) The architecture and function of the light-harvesting apparatus of purple bacteria: from single molecules to in vivo membranes. *Q Rev Biophys* **39** (3), 227–324.
179 Melkozernov AN and Blankenship RE (2003) Structural modeling of the Lhca4 Subunit of LHCI-730 peripheral antenna in photosystem I based on similarity with LHCII. *J Biol Chem* **278** (45), 44542–44551.
180 Pan X, Ma J, Su X, Cao P, Chang W, Liu Z, Zhang X and Li M (2018) Structure of the maize photosystem I supercomplex with light-harvesting complexes I and II. *Science* **360** (6393), 1109–1113.
181 Passarini F, Wientjes E, van Amerongen H and Croce R (2010) Photosystem I light-harvesting complex Lhca4 adopts multiple conformations: red forms and excited-state quenching are mutually exclusive. *Biochim Biophys Acta* **1797** (4), 501–508.
182 Saito K, Kosugi M, Qiu L, Minagawa J and Ishikita H (2025) Identification and design principles of far-red-absorbing chlorophyll in the light-harvesting complex. *J Biol Chem* 108518.
183 Kosugi M, Kawasaki M, Shibata Y, Hara K, Takaichi S, Moriya T, Adachi N, Kamei Y, Kashino Y, Kudoh S *et al.* (2023) Uphill energy transfer mechanism for photosynthesis in an Antarctic alga. *Nat Commun* **14** (1), 730.

184 Wolf BM, Niedzwiedzki DM, Magdaong NCM, Roth R, Goodenough U and Blankenship RE (2018) Characterization of a newly isolated freshwater Eustigmatophyte alga capable of utilizing far-red light as its sole light source. *Photosynth Res* **135** (1), 177–189.
185 Niedzwiedzki DM, Wolf BM and Blankenship RE (2019) Excitation energy transfer in the far-red absorbing violaxanthin/vaucheriaxanthin chlorophyll a complex from the eustigmatophyte alga FP5. *Photosynth Res* **140** (3), 337–354.
186 Batista-Silva W, da Fonseca-Pereira P, Martins AO, Zsögön A, Nunes-Nesi A and Araújo WL (2020) Engineering improved photosynthesis in the era of synthetic biology. *Plant Commun* **1** (2), 100032.
187 Ort DR, Merchant SS, Alric J, Barkan A, Blankenship RE, Bock R, Croce R, Hanson MR, Hibberd JM, Long SP *et al.* (2015) Redesigning photosynthesis to sustainably meet global food and bioenergy demand. *Proc Natl Acad Sci* **112** (28), 8529–8536.
188 Walter J and Kromdijk J (2021) Here comes the sun: How optimization of photosynthetic light reactions can boost crop yields. *J Integr Plant Biol*
189 Leister D (2023) Enhancing the light reactions of photosynthesis: Strategies, controversies, and perspectives. *Mol Plant* **16** (1), 4–22.
190 Li C, Du X and Liu C (2025) Enhancing crop yields to ensure food security by optimizing photosynthesis. *J Genet Genomics*
191 Tosens T, Alboresi A, van Amerongen H, Bassi R, Busch FA, Consoli G, Ebenhöh O, Flexas J, Harbinson J, Jahns P *et al.* (2025) New avenues in photosynthesis: from light harvesting to global modeling. *Physiol Plant* **177** (2), e70198.
192 Chen M and Blankenship RE (2011) Expanding the solar spectrum used by photosynthesis. *Trends Plant Sci* **16** (8), 427–431.
193 Blankenship RE and Chen M (2013) Spectral expansion and antenna reduction can enhance photosynthesis for energy production. *Curr Opin Chem Biol* **17** (3), 457–461.
194 Slattery RA and Ort DR (2021) Perspectives on improving light distribution and light use efficiency in crop canopies. *Plant Physiol* **185** (1), 34–48.
195 Tian J, Wang C, Chen F, Qin W, Yang H, Zhao S, Xia J, Du X, Zhu Y, Wu L *et al.* (2024) Maize smart-canopy architecture enhances yield at high densities. *Nature*
196 Cutolo EA, Guardini Z, Dall'Osto L and Bassi R (2023) A paler shade of green: engineering cellular chlorophyll content to enhance photosynthesis in crowded environments. *New Phytol* **239** (5), 1567–1583.
197 Kirst H, Gabilly ST, Niyogi KK, Lemaux PG and Melis A (2017) Photosynthetic antenna engineering to improve crop yields. *Planta* **245** (5), 1009–1020.
198 Wang Y, Oliver TJ, Croce R and Long SP (2025) Addition of longer wavelength absorbing chlorophylls into crops could increase their photosynthetic productivity by 26%. *Nat Commun* **16** (1), 7933.
199 Zhu XG, Long SP and Ort DR (2008) What is the maximum efficiency with which photosynthesis can convert solar energy into biomass? *Curr Opin Biotechnol* **19** (2), 153–159.
200 Elias E, Brache K, Schäfers J and Croce R (2024) Coloring outside the lines: exploiting pigment–protein synergy for far-red absorption in plant light-harvesting complexes. *J Am Chem Soc* **146** (5), 3508–3520.
201 Elias E, Liguori N, Saga Y, Schäfers J and Croce R (2021) Harvesting far-red light with plant antenna complexes incorporating chlorophyll *d*. *Biomacromolecules* **22** (8), 3313–3322.
202 Cianfarani N, Calcinoni A, Agostini A, Elias E, Bortolus M, Croce R and Carbonera D (2025) Far-red absorbing LHCII incorporating chlorophyll d preserves photoprotective carotenoid triplet–triplet energy transfer pathways. *The Journal of Physical Chemistry Letters* **16** (7), 1720–1728.
203 Bryant DA, Hunter CN and Warren MJ (2020) Biosynthesis of the modified tetrapyrroles-the pigments of life. *J Biol Chem* **295** (20), 6888–6925.
204 Swingley WD, Chen M, Cheung PC, Conrad AL, Dejesa LC, Hao J, Honchak BM, Karbach LE, Kurdoglu A, Lahiri S *et al.* (2008) Niche adaptation and genome expansion in the chlorophyll d-producing cyanobacterium Acaryochloris marina. *Proc Natl Acad Sci* **105** (6), 2005–2010.
205 Ranepura GA, Mao J, Vermaas JV, Wang J, Gisriel CJ, Wei RJ, Ortiz-Soto J, Uddin MR, Amin M and Brudvig GW (2023) Computing the Relative Affinity of Chlorophylls a and b to Light-Harvesting Complex II. *J Phys Chem B* **127** (51), 10974–10986.
206 Mascoli V, Bersanini L and Croce R (2020) Far-red absorption and light-use efficiency trade-offs in chlorophyll f photosynthesis. *Nat Plants* **6** (8), 1044–1053.
207 Renger T, May V and Kühn O (2001) Ultrafast excitation energy transfer dynamics in photosynthetic pigment–protein complexes. *Phys Rep* **343** (3), 137–254.
208 Kühlbrandt W (1994) Structure and function of the plant light-harvesting complex. *LHCII Current Opinion in Structural Biology* **4** (4), 519–528.
209 Sundström V and van Grondelle R (1990) Energy transfer in photosynthetic light-harvesting antennas. *J Opt Soc Am B* **7** (8), 1595–1603.
210 Mascoli V, Novoderezhkin V, Liguori N, Xu P and Croce R (2020) Design principles of solar light harvesting in plants: Functional architecture of the monomeric antenna CP29. *Biochimica et Biophysica Acta (BBA) - Bioenergetics* **1861** (3), 148156.

211 Bricker WP and Lo CS (2014) Excitation energy transfer in the peridinin-chlorophyll a-protein complex modeled using configuration interaction. *J Phys Chem B* **118** (31), 9141–9154.
212 Olbrich C, Strümpfer J, Schulten K and Kleinekathöfer U (2011) Theory and simulation of the environmental effects on FMO electronic transitions. *The Journal of Physical Chemistry Letters* **2** (14), 1771–1776.
213 Häse F, Kreisbeck C and Aspuru-Guzik A (2017) Machine learning for quantum dynamics: deep learning of excitation energy transfer properties. *Chem Sci* **8** (12), 8419–8426.
214 Uauy C, Nelissen H, Chan RL, Napier JA, Seung D, Liu L and McKim SM (2025) Challenges of translating Arabidopsis insights into crops. *Plant Cell*
215 Zhu X-G, Song Q and Ort DR (2012) Elements of a dynamic systems model of canopy photosynthesis. *Curr Opin Plant Biol* **15** (3), 237–244.
216 Croce R, Carmo-Silva E, Cho YB, Ermakova M, Harbinson J, Lawson T, McCormick AJ, Niyogi KK, Ort DR, Patel-Tupper D *et al.* (2024) Perspectives on improving photosynthesis to increase crop yield. *Plant Cell*
217 Song Q, Wang Y, Qu M, Ort DR and Zhu X-G (2017) The impact of modifying photosystem antenna size on canopy photosynthetic efficiency—Development of a new canopy photosynthesis model scaling from metabolism to canopy level processes. *Plant Cell Environ* **40** (12), 2946–2957.
218 Müller K, Siegel D, Rodriguez Jahnke F, Gerrer K, Wend S, Decker EL, Reski R, Weber W and Zurbriggen MD (2014) A red light-controlled synthetic gene expression switch for plant systems. *Mol BioSyst* **10** (7), 1679–1688.
219 Xiao Y, Tholen D and Zhu X-G (2016) The influence of leaf anatomy on the internal light environment and photosynthetic electron transport rate: exploration with a new leaf ray tracing model. *J Exp Bot* **67** (21), 6021–6035.
220 Liu F, Song Q, Zhao J, Mao L, Bu H, Hu Y and Zhu X-G (2021) Canopy occupation volume as an indicator of canopy photosynthetic capacity. *New Phytol* **232** (2), 941–956.
221 Burgess AJ, Retkute R, Herman T and Murchie EH (2017) Exploring relationships between canopy architecture, light distribution, and photosynthesis in contrasting rice genotypes using 3D canopy reconstruction. *Front Plant Sci* 8.
222 Salvatori N, Carteni F, Giannino F, Alberti G, Mazzoleni S and Peressotti A (2022) A system dynamics approach to model photosynthesis at leaf level under fluctuating light. *Front Plant Sci* **12**,
223 Stirbet A, Lazár D, Guo Y and Govindjee G (2019) Photosynthesis: basics, history and modelling. *Ann Bot* **126** (4), 511–537.
224 Buda F (2009) Introduction to theory/modeling methods in photosynthesis. *Photosynth Res* **102** (2-3), 437–441.
225 Gu S, Wen W, Xu T, Lu X, Yu Z, Guo X and Zhao C (2022) Use of 3D modeling to refine predictions of canopy light utilization: A comparative study on canopy photosynthesis models with different dimensions. *Front Plant Sci* (13),
226 Zhu X-G, de Sturler E and Long SP (2007) Optimizing the distribution of resources between enzymes of carbon metabolism can dramatically increase photosynthetic rate: a numerical simulation using an evolutionary algorithm. *Plant Physiol* **145** (2), 513–526.
227 Zhu X-G, Wang Y, Ort DR and Long SP (2013) e-photosynthesis: a comprehensive dynamic mechanistic model of C3 photosynthesis: from light capture to sucrose synthesis. *Plant Cell Environ* **36** (9), 1711–1727.
228 Tholen D and Zhu X-G (2011) The mechanistic basis of internal conductance: a theoretical analysis of mesophyll cell photosynthesis and CO2 diffusion. *Plant Physiol* **156** (1), 90–105.
229 Song Q, Zhang G and Zhu XG (2013) Optimal crop canopy architecture to maximise canopy photosynthetic CO(2) uptake under elevated CO(2) - a theoretical study using a mechanistic model of canopy photosynthesis. *Funct Plant Biol* **40** (2), 108–124.
230 Krüger TPJ, Novoderezhkin VI, Ilioaia C and van Grondelle R (2010) Fluorescence Spectral Dynamics of Single LHCII Trimers. *Biophys J* **98** (12), 3093–3101.
231 Ennist NM, Wang S, Kennedy MA, Curti M, Sutherland GA, Vasilev C, Redler RL, Maffeis V, Shareef S, Sica AV *et al.* (2024) De novo design of proteins housing excitonically coupled chlorophyll special pairs. *Nat Chem Biol* **20** (7), 906–915.
232 Curti M, Maffeis V, Duarte LGTA, Shareef S, Hallado LX, Curutchet C and Romero E (2023) Engineering excitonically coupled dimers in an artificial protein for light harvesting via computational modeling. *Protein Sci* **32** (3), e4579.
233 Ennist NM, Stayrook SE, Dutton PL and Moser CC (2022) Rational design of photosynthetic reaction center protein maquettes. *Front Mol Biosci* **9**, 997295.
234 Ennist NM, Zhao Z, Stayrook SE, Discher BM, Dutton PL and Moser CC (2022) De novo protein design of photochemical reaction centers. *Nat Commun* **13** (1), 4937.
235 Amunts A, Toporik H, Borovikova A and Nelson N (2010) Structure Determination and Improved Model of Plant Photosystem I*. *J Biol Chem* **285** (5), 3478–3486.

236 Kato K, Nagao R, Jiang T-Y, Ueno Y, Yokono M, Chan SK, Watanabe M, Ikeuchi M, Shen J-R, Akimoto S *et al*. (2019) Structure of a cyanobacterial photosystem I tetramer revealed by cryo-electron microscopy. *Nat Commun* **10** (1), 4929.

237 Mazor Y, Borovikova A and Nelson N (2015) The structure of plant photosystem I super-complex at 2.8 Å resolution. *elife* **4**, e07433.

238 Su X, Ma J, Wei X, Cao P, Zhu D, Chang W, Liu Z, Zhang X and Li M (2017) Structure and assembly mechanism of plant C2S2M2-type PSII-LHCII supercomplex. *Science* **357** (6353), 815–820.

239 Sun H, Shang H, Pan X and Li M (2023) Structural insights into the assembly and energy transfer of the Lhcb9-dependent photosystem I from moss Physcomitrium patens. *Nat Plants* **9** (8), 1347–1358.

240 Wang J, Yu L-J, Wang W, Yan Q, Kuang T, Qin X and Shen J-R (2021) Structure of plant photosystem I–light harvesting complex I supercomplex at 2.4 Å resolution. *J Integr Plant Biol* **63** (7), 1367–1381.

241 Wei X, Su X, Cao P, Liu X, Chang W, Li M, Zhang X and Liu Z (2016) Structure of spinach photosystem II-LHCII supercomplex at 3.2 Å resolution. *Nature* **534** (7605), 69–74.

242 Kim E, Lee D, Sakamoto S, Jo J-Y, Vargas M, Ishizaki A, Minagawa J and Kim H (2025) Network analysis with quantum dynamics clarifies why photosystem II exploits both chlorophyll a and b. *Sci Adv* **11** (19), eads0327.